THE SMALL GTPASE RHEB IS REQUIRED FOR SPERMATOGENESIS BUT NOT OOGENESIS

APPROVED BY SUPERVISORY COMMITTEE

_____
Diego Castrillon, MD, PhD

_____
Lawrence Lum, PhD

_____
Rolf Brekken, PhD

_____
James Amatruda, MD, PhD

DEDICATION

Dedicated to Grandpa and Grandma Smith

You made science fun and it has been ever since.

THE SMALL GTPASE RHEB IS REQUIRED FOR SPERMATOGENESIS BUT NOT OOGENESIS

by

MICHAEL DAVID BAKER

DISSERTATION

Presented to the Faculty of the Graduate School of Biomedical Sciences

The University of Texas Southwestern Medical Center at Dallas

In Partial Fulfillment of the Requirements

For the Degree of

DOCTOR OF PHILOSOPHY

The University of Texas Southwestern Medical Center

Dallas, Texas

December, 2013

ACKNOWLEDGEMENTS

First off, I would like to sincerely thank my mentor Diego Castrillon for his support, advice and encouragement. It has been my privilege to learn from you and to be a part of your lab. It is clear that you have a genuine interest in the success of your students and I thank you for the many doors which you have opened for me.

I would also like to express my gratitude to my dissertation committee: Drs. Lawrence Lum, Rolf Brekken and James Amatruda. Your valuable insights into my project provided focus and clarity. Additionally, I would like to thank the entire Genetics and Development faculty for cultivating an environment rich in learning, discussion and collaboration.

Each member of the Castrillon lab (Gina Aloisio, Mohammad Ezzati, Edward Tarnawa, Zhuoru Wu, Yuji Nakada, Ileana Cuevas, Christopher Peña, Jishnu Mukherjee and Duygu Saatcioglu) significantly contributed to this work. You all made work truly enjoyable but most of all I appreciated the occasional adventures that greatly helped relieve the daily stresses of science.

I have had the pleasure of enduring graduate school alongside a handful of remarkable people (Ryan Carsens, Bethany Weigle, Mandy Wong, Sarah Gonzales, Leilani Marty-Santos, Marieke Burleson, Nida Iqbal, Steven Harrison, Ankit Garg and Arnaldo Carreira). I hope you all accomplish your dreams. Keep in touch.

I am also blessed to be near an amazing group of friends who have grown as close as family (Tim, Katie, Luke, Juliana, Stephen, Nathan, Rachel, Dan, Amy, and Ashley). Thank you for your support and distraction.

A brief mention of my family (and that includes the in-laws!) does not begin to convey the importance of their unconditional love, encouragement and support. It has been priceless to have them so close for the past four years. Mom and Dad, thank you.

And finally, my deepest thanks to my wife Devynn and my son Grayson. You have been and continue to be my motivation to press on when things look tough. I could not have done this without you.

THE SMALL GTPASE RHEB IS REQUIRED FOR SPERMATOGONIAL BUT NOT OOGENESIS

MICHAEL DAVID BAKER

The University of Texas Southwestern Medical Center at Dallas, 2013

DIEGO H. CASTRILLON, M.D., Ph.D.

The process of germ cell development is under the tight control of various signaling pathways among which the PI3K-PKB-mTOR pathway is of critical importance. Previous studies have demonstrated sex-specific roles for several components of this pathway. In the current study I aimed to evaluate the role of Rheb, a member of the small GTPase superfamily and a critical component for mTORC1 activation, in male and female gametogenesis. The function of Rheb in development and the nervous system has been extensively studied, but little was known about its role in the germline. I have exploited genetic approaches in the mouse to study the role of Rheb in the germline and have identified an essential role in spermatogenesis. Conditional knockout (cKO) of *Rheb* in the male germline resulted in severe oligoasthenoteratozoospermia and male sterility. More detailed phenotypic analyses uncovered an age-dependent meiotic progression defect combined with subsequent abnormalities in spermiogenesis as evidenced by abnormal sperm morphology. In the

female, however, germ-cell specific inactivation of *Rheb* was not associated with any discernible abnormality; these cKO mice were fertile with morphologically unremarkable ovaries, normal primordial follicle formation, and subsequent follicle maturation. The absence of an abnormal ovarian phenotype is striking given previous studies demonstrating a critical role for the mTORC1 pathway in the maintenance of primordial follicle pool. In conclusion, our findings demonstrate an essential role of *Rheb* in diverse aspects of spermatogenesis but suggest the existence of functionally-redundant factors that can compensate for *Rheb* deficiency within oocytes.

TABLE OF CONTENTS

PRIOR PUBLICATONS

Baker MD, Aloisio GM, Tarnawa ED, Ezzati M, Cuevas I, Nakada Y, Worley PF & Castrillon DH 2013 The small GTPase Rheb is required for spermatogenesis but not oogenesis. *Submitted, under review.*

Tarnawa ED, **Baker MD**, Aloisio GM, Carr BR & Castrillon DH 2013 Gonadal expression of foxo1, but not foxo3, is conserved in diverse Mammalian species. *Biol Reprod* 88 103.

Du L, Subauste MC, DeSevo C, Zhao Z, **Baker MD**, Borkowski R, Schageman J, Greer R, Yang C, Suraokar M, Wistuba II, Gazdar AF, Minna JD & Pertsemlidis A 2012 miR-337-3p and its targets *STAT3* and *RAP1A* modulate taxane sensitivity in non-small cell lung cancers. *PLoS ONE* 7 e39167.

LIST OF FIGURES

LIST OF TABLES

LIST OF ABBREVIATIONS

ATP: adenosine triphosphate

BTB: blood-testis barrier

cKO: conditional knock out

DNA: deoxyribonucleic acid

E: embryonic

FSH: follicle-stimulating hormone

GC: granulosa cell

GCNA: germ cell nuclear antigen

GDNF: glial cell derived neurotrophic factor

GnRH: gonadotropin-releasing hormone

H&E: hematoxylin & eosin

IHC: immunohistochemistry

LH: Luteinizing Hormone

mTOR: mammalian target of rapamycin

PBS: phosphate buffered saline

PCR: polymerase chain reaction

PD: post-natal day

PF: primordial follicle

PFA: primordial follicle activation

pH3: phospho-histone H3

PI3K: phosphoinositide 3-kinase

PKB: protein kinase B (also known as AKT)

PTEN: phosphatase and tensin homologue deleted on chromosome 10 xix

RA: retinoic acid

RIN: rna integrity number

RNA: ribonucleic acid

RTK: receptor tyrosine kinase

SC: synaptonemal complex

SRY: sex-determining region Y

SSC: spermatogonial stem cell

TAM: tamoxifen

TGCT: testicular germ cell tumor

TSC: tuberous sclerosis

TUNEL: terminal deoxynucleotidyl transferase dUTP nick end labeling

WT: wild-type

ZP: zona pellucida

CHAPTER ONE

Introduction

SEXUAL REPRODUCTION AND GAMETEOGENESIS

Introduction

The sperm and egg are together an elegantly designed solution to the complex set of criteria required for sexual reproduction. There are multiple theories attempting to explain the evolution of sexual reproduction though they have proven difficult to empirically test. The promotion of genetic variation as a result of homologous recombination is perhaps the most widely accepted of these theories (de Visser & Elena 2007). This variation allows for reproductive competition between genetically unique offspring and gives the species the greatest opportunity to thrive in a volatile environment where the ideal genotype for the offspring cannot be predetermined. Other theories weigh the benefits of sexual reproduction as a mechanism for increased parasite resistance (Hamilton *et al.* 1990) or clearance of deleterious mutations (Kondrashov 1988). However, with any provided benefit of sexual reproduction come a number of challenges that have heavily influenced the development of the male and female gametes.

The first requirement of sexual reproduction is the division of the genome. From *Drosophila* to humans, the formation of a haploid gamete has only been successful through the process of meiosis, a replication of the diploid genome followed by two reductional divisions. It has been suggested that this mechanism arose as a variation on the DNA repair machinery of mitosis; however, the multiple novel meiotic specific events constitute a large evolutionary leap for the early eukaryote. It is for this reason that

meiosis was regarded by W.D. Hamilton as one of the most difficult evolutionary problems (Hamilton 2001, Wilkins & Holliday 2009).

The second seemingly-obvious, yet far from trivial, requirement is the transportation of each gamete to the site of fertilization of which the sperm takes the majority of the responsibility. The motile sperm is guided by both thermotaxic and chemotaxic signals of the female reproductive tract all the while combating the harsh conditions of the voyage as well as the obstacles of the cervix and fallopian tubes (Bahat & Eisenbach 2006, Eisenbach & Giojalas 2006). The motility of most sperm has been accomplished by the use of the flagella, a specialized cilia motor which propels the sperm towards the egg (Inaba 2011). The amoeboid sperm of the nematode provides one rare exception which, through the use of a single pseudopod, crawls to the egg (Fraire-Zamora & Cardullo 2010). The small size and motility of the sperm has come to be the fundamental definition of the male sex whereas the female is designated by the larger of the two gametes.

To increase the likelihood of a fertilization event most species have employed a "quantity over quality" strategy, producing an impressive excess of sperm which often outnumber eggs by several orders of magnitude (Parker 1982, Parker & Pizzari 2010). These sperm are simplified to only the most essential components (haploid genome, acrosome, mitochondria and flagella) to allow for the mass production of gametes with as little energy investment as possible (Alberts *et al.* 2002). On the other hand, *Drosophilids* are well-known for their large sperm; the giant sperm of *Drosophila bifurca* measures over twenty times the length of the fly itself and only barely outnumber the eggs by a ratio of less than 6 to 1 (Bjork *et al.* 2007). The reduced size and subsequent limited nutrient supply of the sperm has caused the egg to respond with a compensatory increase in size as the energy, proteins and RNAs required for early embryo development are almost completely provided by the egg (Randerson & Hurst 2001).

The temporal alignment of male and female gamete production introduces some of the largest differences in sexual reproduction between species. In all known species sperm production is continually fueled by a self-renewing stem cell population. The female, however, has developed several unique solutions to regulating oocyte production to maximize reproductive potential. Where oocytes are produced from an unlimited stem cell pool in organisms such as *Drosophila*, other species such as the human female produces a constant but limited supply of oocytes which are released gradually over the reproductive years of the organism. This pulsatile ovulation is typically cyclical as, in the absence of progesterone, estradiol levels reach a threshold triggering a release of gonadotropin-releasing hormone (GnRH) from the hypothalamus. GnRH signals to the anterior pituitary to produce luteinizing hormone (LH) which ultimately causes follicular maturation and ovulation (Sherman & Korenman 1975). Further conservation of oocytes has lead to the induced ovulation observed in species such as felines and camelids. Induced ovulators do not release the oocyte until a copulatory signal is received, either through physical stimulation or ovulation-inducing factors found in the seminal plasmid (reveiwed in Adams & Ratto 2013). In several species where isolation limits mating or fertilization until the spring season, the long term storage of sperm extends the reproductive effect of relatively infrequent mating events (Holt 2011).

The final obstacle in the completion of sexual reproduction is the fusion of the two haploid gametes which defines the moment of fertilization. In mammals, the sperm and the egg have specialized structures for fertilization: the zona pellucida (ZP) and acrosome respectively. The ZP is an extracellular matrix consisting mainly of the glycoproteins ZP1, 2, 3, and 4. These four proteins facilitate sperm binding and trigger the release of digestives enzyme, including hyaluronidases and acrosin, from the sperm acrosome (Dean 1992). In non-mammalian animals a structure similar to the zona pellucida, called the vitelline layer, plays an important role in the attraction as well as

activation of the sperm to prevent inter-species fertilization, especially important when eggs are fertilized outside of the body (e.g. fish) (Hirohashi & Lennarz 2001). In this context these phylogenetically-complex details of gametogenesis provide an unending source of questions for scientific investigation.

Assembly of the primordial follicle

The ovary is the oocyte producing organ and consists of three main cell types (oocytes, granulosa cells, and theca cells) which form a cluster of growing follicles of all stages of development (**Fig. 1.1**). Differentiation of the ovary is first distinguishable from the testis on the twelfth day post-coitus, known as embryonic day 12 (E12), as the primordial germ cell commits to oocyte development and the somatic support cell precursors begin to differentiate into granulosa cells (Yao *et al.* 2002). This developmental pathway is chosen by default in the absence of a Y chromosome containing the transcription factor *Sry* (Sex-determining region Y), expression of which deters the somatic cells of the gonad from their granulosa cell fate and drives Sertoli cell development (Maatouk & Capel 2008). The pre-granulosa cells and oogonia continue to multiply via mitosis until shortly after birth. By post-natal day 3 (PD3), the oogonia have reached prophase I of meiosis, however, the oocyte will enter quiescence before the first division. At this point they are surrounded by granulosa cells forming the finite pool of primordial follicles that will define the reproductive life span of the female mouse (**Fig. 1.2**). The primordial follicle remains quiescent until they undergo primordial follicle activation (PFA) (Alberts *et al.* 2002).

Follicle activation and growth

The initiation of primordial follicle activation remains poorly understood despite the identification of multiple genes required for the repression of PFA (see Chapter 2 for

in-depth discussion of PFA regulation). The signal responsible for PFA regulation likely originates from the somatic cells of the ovary and while several lines of evidence implicate Kit and Kit-Ligand (Parrott & Skinner 1999, Adhikari & Liu 2009, McLaughlin & McIver 2009), Kit signaling, at least via the PI3K pathway, has been shown to be dispensable for PFA (John *et al.* 2009). Regardless of the source, the signal maintains a delicate balance of follicle activation and quiescence which preserves the follicle pool for the organism's entire lifetime. As this constant supply of activated follicles irreversibly commits to ovulation or atresia, the flattened squamous granulosa cells change shape into a single layer of cuboidal cells surrounding the growing oocyte (Alberts *et al.* 2002).

The primary follicle resumes meiosis; yet, the first division will not be completed till the day before ovulation. The primary follicle then transitions to the secondary follicle stage while the oocyte continues to rapidly increase in size and the granulosa cells proliferate forming multiple layers (Alberts *et al.* 2002). At this point, follicle stimulating hormone (FSH) rescues the growing follicles from an otherwise atretic death and promotes further follicular growth. As the secondary follicle increases in size it is termed pre-antral, and upon the appearance of the antrum (a fluid-filled cavity adjacent to the oocyte), the final stage of follicular growth is reached--the antral follicle (Alberts *et al.* 2002). Ovulation occurs in response to a surge of luteinizing hormone (LH) produced in the anterior pituitary and received by granulosa cells immediately prior to estrus. After the mature oocyte is released from its surrounding granulosa cells, the remaining follicle forms the corpora lutea which temporarily produces high levels of progesterone preparing the endometrium of the uterus for embryo implantation. In the event of fertilization and implantation the corpora lutea will continue to produce progesterone to maintain the pregnancy, otherwise it will degenerate and form a corpus albicans, a mass of fibrous scar tissue (Alberts *et al.* 2002).

Testis development and organization

The testis is comprised of a tightly packed circuit of sperm producing ducts called the seminiferous tubules. Four main cell types form the structure of the testis: germ cells, Sertoli cells, Leydig cells and myoid cells. The contractile peritubule myoid cells form a single layer of cells surrounding the seminiferous tubules and are in intimate contact with the external aspect of the basement membrane. Along this basement membrane lie the undifferentiated spermatogonia as well as the Sertoli cells. The Sertoli cells completely surround the developing germ cells and form the blood-testis barrier (BTB) which divides the tubule into the basal compartment, which contains the undifferentiated spermatogonia, and the adluminal compartment which contains spermatocytes, spermatids, and spermatozoa (Alberts *et al.* 2002). This barrier is essential to isolate developing sperm from initiating an auto-immune response. In the event of traumatic injury and breach of the BTB, the ensuing immune response can lead to male infertility. The BTB is also instrumental in conferring cellular polarity during spermiogenesis (Wong & Cheng 2005). The Leydig cells fill the spaces surrounding the tubules and are the predominant source of testosterone, which is required by Sertoli cells for spermatogenesis and has an effect on multiple other tissues responsible for the male secondary sex characteristics. A cross section of the testis exposes the organization of the seminiferous tubule (**Fig. 1.3**).

As previously mentioned, embryonic testis development hinges on the expression of *Sry*, the sex determining gene found on the Y chromosome. Deletion of *Sry* results in a complete sex reversal phenotype (Maatouk & Capel 2008). *Sry* is expressed in the somatic cells of the embryonic testis at around E11 and functions as a transcription factor initiating Sertoli cell development through the regulation of *Sox9* (Maatouk & Capel 2008, Sekido 2010). The Sertoli cell subsequently initiates the development of the prospermatogonia (a.k.a. gonocytes) as well as the Leydig cells. At birth, the primitive

spermatogonia are already contained in the lumen of the seminiferous tubules. During the first days of life the spermatogonia migrate to the basement membrane and rapidly divide to form the pool of spermatogonia stem cells that will provide a continuous supply of sperm for the entire adult life of the male (Alberts *et al.* 2002).

Spermatogonial stem cell maintenance and differentiation

SSCs have proven difficult to identify based on the lack of known SSC markers. While some markers are limited to a subset of spermatogonial cell types (**Fig 1.4**), the lack of specifically expressed proteins makes it impossible to purify the SSC from the remaining undifferentiated spermatocyte population. Despite this challenge much has been learned through the use of the genetic approaches, SSC transplantation assays, and the development of long-term SSC culture conditions. A long list of SSC expressed genes have been shown to be indispensable in maintaining the balance between SSC self-renewal and differentiation (reviewed in Phillips et al 2010). At the heart of the SSC regulation lie Plzf, Taf4b, and GDNF (which upregulate the transcription factors bcl6b, etv5, and lhx1). The PI3K/PKB/FOXO1 is also of critical importance in the regulation of SSC self-renewal and differentiation. The loss of Foxo1 was shown to cause a decrease in testis size where seminiferous tubules either exhibited a lack of differentiating spermatogonia or the spermatogonia were missing altogether (Goertz *et al.* 2011).

As the SSC, a sub-population of the undifferentiated spermatogonia, enters the proliferative phase of spermatogenesis, it undergoes multiple rounds of mitosis with incomplete cytokinesis resulting in chains of spermatogonia, connected by cytoplasmic bridges (**Fig. 1.5**). The single undifferentiated spermatogonia are termed A_{single}, a pair is A_{paired}, and a chain of 4 to 16 cells is $A_{aligned}$. As the spermatogonia initiate differentiation they form type B spermatogonia. The type B spermatogonia transition to spermatocytes as the cell initiates meiosis (Jan *et al.* 2012).

Meiosis is regulated at multiple levels to ensure genetic fidelity

Meiotic entry is dependent on a complex transcriptional program which is promoted through the controlled exposure of the germ cells to retinoic acid (RA) (Childs *et al.* 2011). Vitamin A, the RA precursor, was identified early on as an essential signaling molecule for meiosis progression (Thompson *et al.* 1964) yet recent efforts have only begun to elucidate downstream effect of this signaling molecule. RA binds the RA-receptor which heterodimerizes with the retinoid-X-receptor to recognize RA response elements in the promoters of target genes. A downstream transcription factor, Stimulated by Retinoic Acid 8 (*Stra8*), is upregulated in response to retinoic acid (Oulad-Abdelghani *et al.* 1996). The function of Stra8 remains unclear but the answer likely lies within the gene targets regulated by Stra8. The prospermatogonia of the embryonic testis are protected from RA as the Sertoli cells express Cyp26B1, the RA-metabolizing enzyme. The embryonic ovary however does not express this enzyme, and hence, oocytes are "unprotected". Consequently, in the ovary, meiosis initiates before birth (Childs *et al.* 2011). As the spermatocyte initiates meiosis the condensation and pairing of chromosomes leads to the formation of the synaptonemal complex (SC). The SC functions as a scaffold for the homologous recombination machinery which exchanges genetic material across sister chromatids (Fraune *et al.* 2012). This recombination serves as one of the most important checkpoints of meiosis as machinery typically used for DNA-damage repair is used to sense recombination between the sister chromosomes, ensuring proper DNA replication, chromosome pairing and genetic variation (Longhese *et al.* 2009).

The complete transformation of spermiogenesis

After the completion of meiosis, the spermatocyte undergoes the complex morphogenesis which transforms the round spermatid into the elongated spermatid (complete with acrosome, flagella, and condensed nucleus), known as spermiogenesis. Spermiogenesis has been traditionally divided into the Golgi phase, the cap phase, the formation of the tail, and the maturation stage. During the Golgi phase, the round spermatid develops polarity as the cell begins elongation and the mitochondria migrate to the distal centriole initiating formation of the axoneme, the core component of the flagella (Kierszenbaum 2002). Simultaneously, the Golgi body produces the proteolytic enzymes contained in pro-acrosome granules (Abou-Haila & Tulsiani 2000). During the cap phase, the pro-acrosome granules fuse into a single acrosome vesicle which spreads over the anterior pole of the nuclear membrane (Fawcett 1975). The flagellum is assembled as the axoneme elongates assisted by the manchette, a transient microtubule structure (Wolosewick & Bryan 1977). Finally, the DNA is tightly packaged into the condensed nucleus that forms the bulk of the sperm head. This tight condensation is made possible through the use of small arginine-rich proteins call protamines which are specifically expressed during late spermatogenesis (Balhorn 2007).

The release of the mature spermatozoa

The completion of spermatogenesis occurs once the mature spermatozoa are released into the lumen of the seminiferous tubule, a process known as spermiation. The initiation of spermiation occurs as the spermatid releases the extra cytoplasm known as the residual body. The residual body is then phagocytosed by the Sertoli cell (Kerr & de Kretser 1974). Additionally, the adhesion molecules which form the tight Sertoli–germ cell actin-based adherens junction are removed, allowing for the retraction of the Sertoli cell cytoplasm (O'Donnell *et al.* 2011). Finally, the mature spermatozoa disengage from

the epithelium and are then transported to the rete testis on its way to the epididymis where it is concentrated and stored for ejaculation.

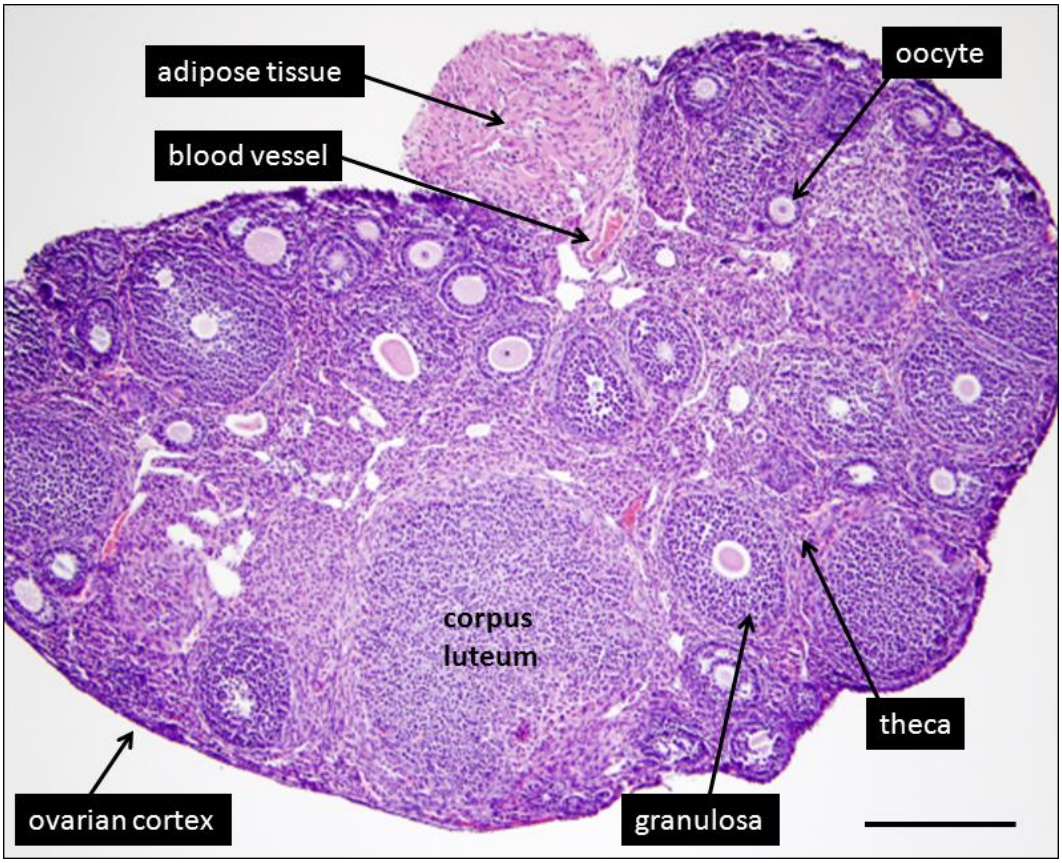

Figure 1.1) The structure of the ovary. An H&E-stained cross section of an adult mouse ovary. The ovary contains quiescent and growing follicles. The oocyte is surrounded by granulosa cells which proliferate as the oocyte matures and grows. The quiescent primordial follicles are typically found along the ovarian cortex but are too small to distinguish at this magnification. Bar = 250 microns.

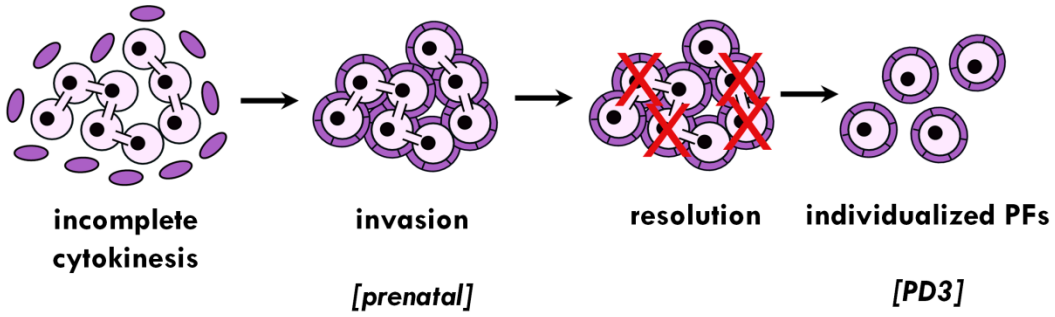

Figure 1.2) Primordial follicle formation and individualization in the neonatal ovary. In the embryonic ovary, oogonia mitotic divisions occur with "incomplete cytokinesis", resulting in clusters of oocytes connected by intercellular bridges. These clusters then become invaded by specialized somatic cells destined to become granulosa cells. The intercellular bridges are then broken down, resulting in individual, physically separate primordial follicles each consisting of a single oocyte and a surrounding layer of granulosa cells.

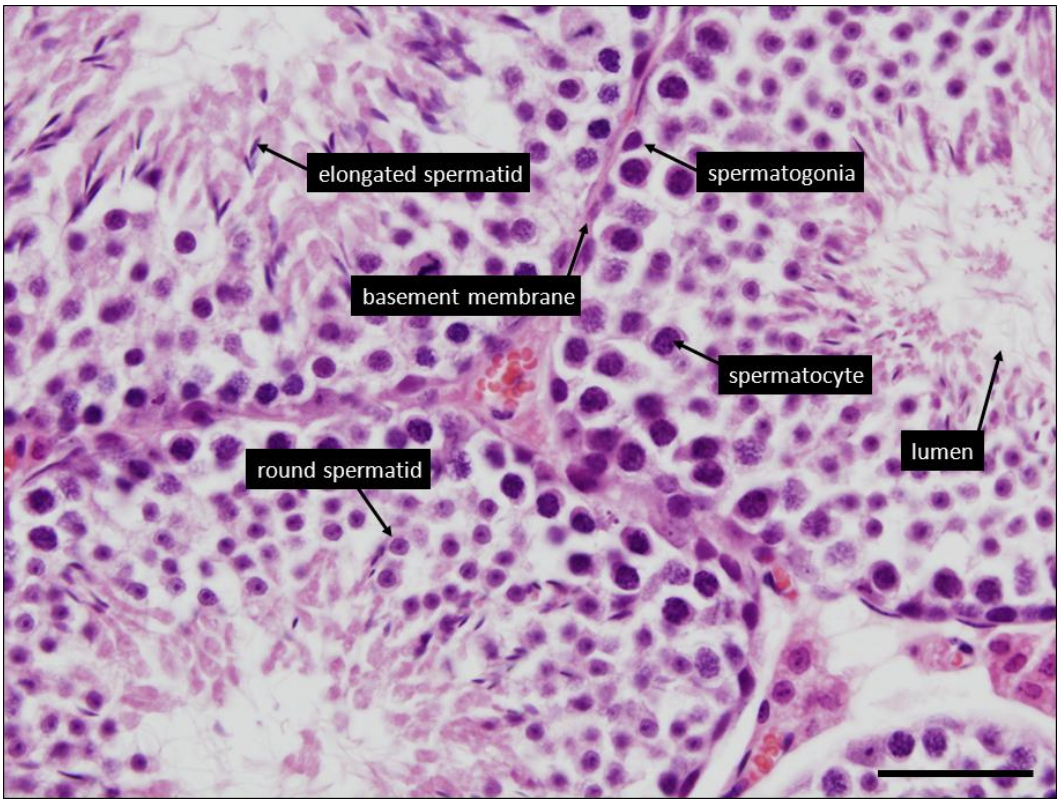

Figure 1.3) Organization of the seminiferous tubule. This high magnification photomicrograph of an H&E-stained adult mouse testis shows three seminiferous tubules surrounding a blood vessel. Key structures such as the basement membrane and tubule lumen are labeled as well as the four classifications of developing germ cells (i.e. spermatogonia, spermatocytes, round and elongating spermatids). Bar = 25 microns.

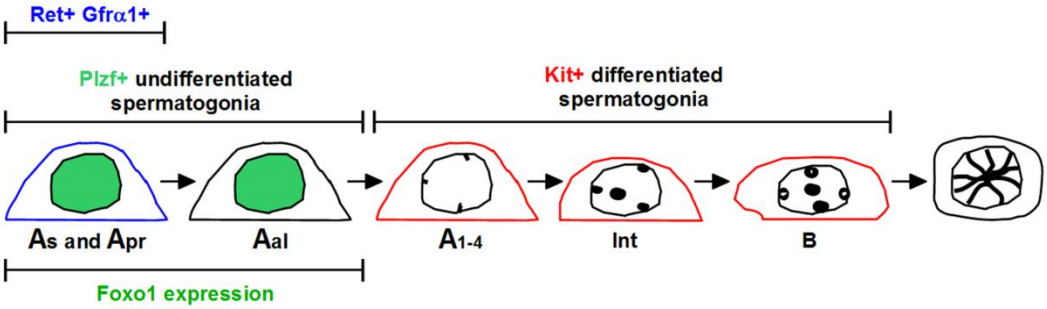

Figure 1.4) Gene expression markers aid in the enrichment, but not identification, of SSCs. While no SSC specific marker has yet to be discovered, many proteins are limited to a subset of spermatogonia. Ret and Gfrα are the most limited marker to date. However, not all Ret^{+} or $Gfr\alpha^{+}$ cells maintain stem cell function. Foxo1 and Plzf label a subset of A_{single} to $A_{aligned}$. Upon differentiation the Kit receptor is expressed, and can be used to negatively select for an SSC enriched population of cells.

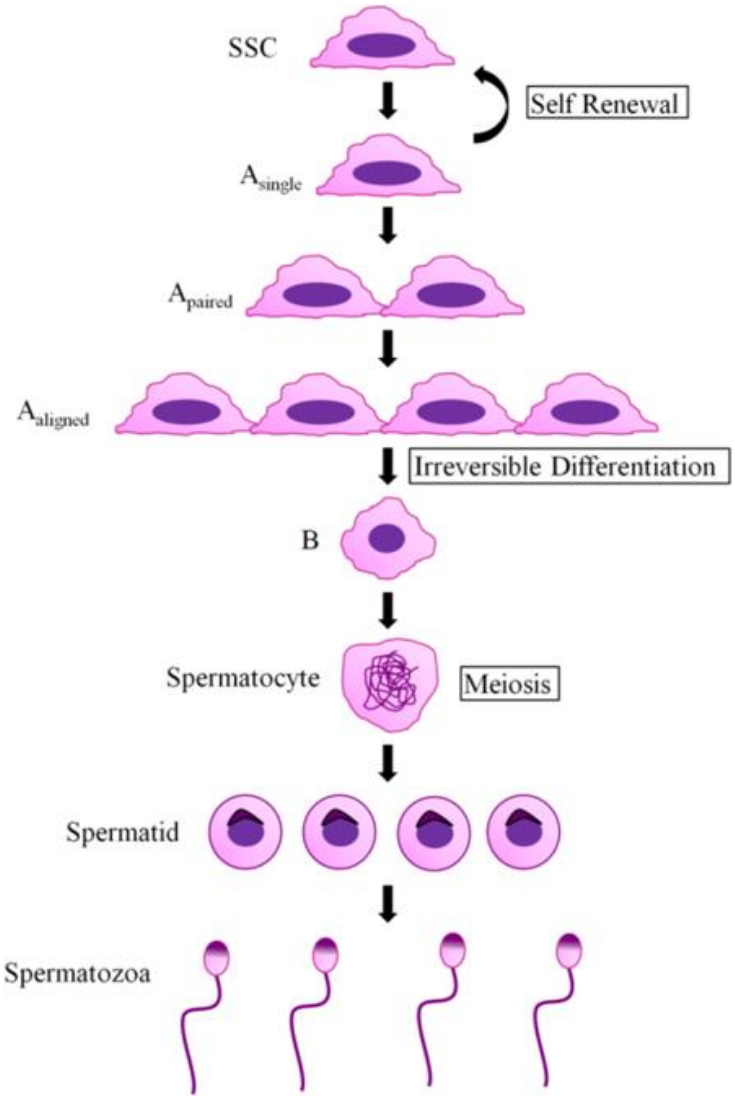

Figure 1.5) Illustration of spermatogenesis. As the SSC mitotically proliferates it gives rise to the A_{single}, A_{paired}, and $A_{aligned}$ undifferentiated spermatogonia. These cells can then either differentiate into type B spermatogonia or continue to function as SSCs. As the type B spermatogonia initiates meiosis it is termed a primary spermatocyte, which undergoes two sequential meiotic divisions resulting in four round spermatids per starting primary spermatocyte. The acrosome vesicles fuse and surround the anterior pole of the spermatid nuclease followed by spermatid elongation and the release of the mature spermatozoa into the lumen of the seminiferous tubule.

CHAPTER TWO

Introduction

PI3K PATHWAY AND FOXO FORKHEAD TRANSCRIPTION

PI3K/PKB/mTOR signaling regulates cell growth and survival

The PI3K/PKB/mTOR signaling pathway is highly conserved among diverse species and plays important roles in the regulation of cell growth. Among other functions, this pathway serves as a key mediator for cellular responses to both the environment and the intracellular milieu, including growth factors, nutrient availability, oxygen levels and intracellular energy charge (Laplante & Sabatini 2009). Working through this pathway, these environmental and intracellular signals exert many changes in cellular physiology to maintain homeostasis. Among these, changes in the rate of protein translation and turnover, and cell cycle progression, are among the best characterized (Laplante & Sabatini 2009).

The cell survival and growth kinase PI3K represents one important node of this pathway. PI3K converts membrane bound phosphatidylinositol 4,5-bisphosphate (PIP2) to phosphatidylinositol (3,4,5)-trisphosphate (PIP3). PIP3 acts as a second messenger by membrane-recruitment and activation of the serine-threonine kinase PKB. Pten, a powerful inhibitor of PI3K signaling, acts to convert PIP3 back to PIP2, thereby suppressing PKB activation. PKB (also known as AKT) in turn phosphorylates and thereby inhibits Tsc2, and also phosphorylates many additional downstream targets including the Foxo transcription factors, which also play multiple roles in cell growth and proliferation (John *et al.* 2008, Goertz *et al.* 2011, Tzivion *et al.* 2011). The AMP kinase AMPK is another important node of this pathway acting via Tsc2. AMPK is activated by

energy stress/low nutrient levels (which result in high intracellular levels of AMP) and also phosphorylates Tsc2. Tsc2 can also be phosphorylated by additional kinases (e.g. Redd1, Erk, Ikkβ) in response to other environmental cues (Laplante & Sabatini 2009). Tsc2 and its physical partner, Tsc1 are structurally unrelated, but form an obligate complex whose principal (and indeed, only well-documented) role is as negative regulator (via Rheb) of mTORC1 (one of the two physically and functionally distinct signaling complexes in which mTOR is a key component, the other being mTORC2). The only known function of Tsc1 is to stabilize Tsc2 and prevent its degradation.

Rheb is required for PI3K/PKB/mTOR regulation of translation

Rheb is a small GTPase and member of the Ras family and is ubiquitously expressed in mammals. Tsc2 contains a GAP (GTPase-activating) domain that stimulates the intrinsic GTPase activity of Rheb, thereby promoting the conversion of Rheb-GTP into Rheb-GDP. Whereas Rheb-GTP potently activates mTORC1, Rheb-GDP is inactive. Rheb directly activates mTORC1 through mechanisms that are not well-understood. These findings are based on numerous genetic and biochemical studies performed in vertebrate and vertebrate model systems and appear to be universal. For example, in *Tsc1* or *Tsc2* mutant cells, mTORC1 is constitutively active, potently stimulating cell growth (Fingar & Blenis 2004, Zou *et al.* 2011).

mTORC1 regulates protein translation largely through two proteins that are key components of the translational control machinery, ribosomal protein S6 (S6) and 4E Binding Protein (4EBP), to potently drive protein translation and cell growth. Phosphorylation of p70S6 kinase (S6K) results in the activation of S6, which allows for the formation of the mRNA translation machinery. mTORC1 also increases protein synthesis by inactivating the translational repressor 4EBP which binds to and inhibits the eukaryotic translation initiation factor 4E (eIF4E) (Laplante & Sabatini 2009).

PI3K/PKB/mTOR plays an important role in both spermatogenesis and oogenesis

Several studies have implicated key components of the PI3K/PKB/mTOR pathway in spermatogenesis and oogenesis. Foxo1 is specifically expressed in undifferentiated spermatogonia, and the three Foxos together regulate multiple steps of spermatogenesis including stem cell maintenance and differentiation (Goertz *et al.* 2011, Tarnawa *et al.* 2013). *Pten* is also required for spermatogenesis; its inactivation with the germline-specific *Vasa-Cre* (Gallardo *et al.* 2007) results in severe defects in spermatogonial maintenance and differentiation, at least in part through Foxo1 (Goertz *et al.* 2011). Other studies have implicated mTORC1 as a regulator of spermatogenesis and spermatogonial stem cell maintenance (Hobbs *et al.* 2010).

In the ovary, *Foxo3* is specifically expressed in primordial follicles, where it serves to potently restrain their activation. In *Foxo3*-null mice, primordial follicles develop normally, but undergo global activation immediately after they are formed, resulting in a syndrome of deregulated follicle growth that results in premature female infertility (Castrillon *et al.* 2003, Hosaka *et al.* 2004, John *et al.* 2007, John *et al.* 2008). Strikingly, an identical ovarian phenotype occurs following conditional germline inactivation of three other PI3K/PKB/mTOR pathway components: *Pten*, *Tsc1*, and *Tsc2*, underscoring the importance of this pathway in the maintenance of the female germline (John *et al.* 2008, Reddy *et al.* 2008, Adhikari *et al.* 2009, Adhikari *et al.* 2010). *Pten* inactivation results in global PFA as the hyperactivation of PKB results in the phosphorylation and cytoplasmic sequestration/inactivation of Foxo3 (John *et al.* 2008). *Tsc1* and *Tsc2* inactivation in oocytes results in global primordial activation associated with mTOR pathway hyperactivity and increased phosphorylation of S6K and 4EBP within oocytes (Adhikari *et al.* 2009, Adhikari *et al.* 2010). These recent mouse models have laid the groundwork for uncovering the regulation of primordial follicle maintenance but further investigations are required to identify how these canonical PI3K branch components

(Pten, PKB, Foxos) interact with canonical mTOR branch components (Tsc1/Tsc2) (Sullivan & Castrillon 2011).

The Ras/Raf/MEK/ERK signaling pathway also controls cell growth and survival through translational and transcriptional regulation

In addition to the PI3K/PKB/mTOR signaling pathway, the Ras/Raf/MEK/ERK pathway plays an essential role in many of the same biological processes (i.e. cell growth, differentiation and apoptosis) (Kolch 2000). The receptor tyrosine kinases (RTKs) which drive PI3K signaling are also capable of activating Ras as well. Once triggered by the respective growth factor, the cytoplasmic domain of the RTK is phosphorylated allowing for recruitment of growth factor receptor-bound protein 2 (Grb2). Grb2 then binds to and activates Son of Sevenless (SOS), a guanine nucleotide exchange factor, which promotes the GDP to GTP exchange that activates Ras and the kinase cascade that phosphorylates Raf, MEK and ERK in rapid succession (Chang *et al.* 2003). This ultimately results in regulation of proliferation, differentiation, apoptosis functions through the regulation of gene expression at both the transcriptional and translational level (Chang *et al.* 2003). The nature of these cellular processes place both Ras/Raf/MEK/ERK and PI3K/AKT/mTOR signaling at the heart of both cancer and stem cell biology.

Regulation of Ras/Raf/MEK/ERK signaling pathway by protein-protein interactions and/or alternative phosphorylation sites.

With multiple upstream receptors as well as downstream effectors, Ras serves as a critical hub for the propagation of several different signals. While the canonical Ras signaling pathway appears relatively straightforward, it has multiple levels of regulation which steer the strength and direction of the signal. The *Ras* gene family consists of four isoforms, *H-Ras*, *N-Ras*, and *K-Ras* (coding for two splice variants K-Ras 4A and K-Ras

4B), which maintain approximately 80% similarity in amino acid sequence while reserving differences for a highly variable region of their C-terminal domains. This inter-isoform variation however is highly conserved between vertebrate species, indicating an unique functional role for each protein (Castellano & Santos 2011). Each isoform is nearly ubiquitously expressed; however, expression levels vary depending on tissue type and developmental stage further supporting the hypothesis of isoform specific activity.

Raf is key regulatory node of the pathway, serving as a target for both ERK-mediated negative feedback and PKA-mediated cyclic AMP sensing (Dhillon *et al.* 2002, Fritsche-Guenther *et al.* 2011). The Raf kinase family consists of A-Raf, B-Raf, and C-Raf. Phosphorylation at five sites, Ser338, Tyr340/341, Thr491, and Ser494, is required for Raf activation. Several additional phosphorylation sites are modified directly by ERK after mitogenic stimulation in a negative feedback loop which disrupts the Ras/Raf interaction to prevent further stimulation (Dougherty *et al.* 2005). The Raf proteins also boast a long list of associated proteins which aid in the down regulation of Raf activity and the recycling of Raf to the activation competent state (reviewed in Kolch 2000).

MEK is perhaps the least regulated member of the pathway though it does provide an additional target for the negative feedback activity of ERK. As activated ERK is stimulating cell survival and proliferation, it also serves to deactivate both Raf and MEK through hyper phosphorylation. Similarly to Raf, hyperphosphorylation by ERK reduces activity further preventing persistent signaling which contributes to the oncogenic process (Dhillon *et al.* 2007). The regulation of ERK is largely controlled by the availability of a long list of ERK substrates, however, required scaffolding proteins and subcellular localization of ERK can prevent the MEK/ERK interaction that provides an additional level of regulation (McKay & Morrison 2007).

Interactions between the Ras/Raf/MEK/ERK and PI3K/PKB/mTOR pathways

Several points of cross-talk between the Ras/Raf/MEK/ERK and PI3K/PKB/mTOR pathways allow for the integration of multiple extracellular signals. This cooperation between the two pathways is necessary to providing the appropriate biological response in response to those environmental cues (reviewd in Mendoza *et al.* 2011). It is important to note that while many agonists are shared between the two pathways, differences in the ligand/receptor affinity provide varying signal intensities as well as durations. For example, insulin and IGF-1 are relatively modest activators of the Ras pathway but serve as potent activators of PI3K signaling (Clerk *et al.* 2006). (Vander Haar *et al.* 2007). Just as activators are shared between the two pathways, several effectors are shared as well. The two pathways partially converge as ERK and mTOR phosphorylate RSK and S6K, respectively. RSK and S6K, as well as PKB, have an affinity to phosphorylate the same RXRXXS/T which can be found in nearly 14,000 proteins (Yaffe *et al.* 2001). This shared substrate promiscuity leads to the activation or repression of many of the same cytoplasmic targets and transcriptional regulators which co-regulate cellular processes including translation and metabolism (e.g. S6, Foxo transcription factors, GSK3, and BAD) (Mendoza *et al.* 2011).

Cross-talk between the core signaling proteins works to either repress or activate the analogous pathways, once again depending on the nature of the signal and the cellular context. Several members of the PI3K/PKB/mTOR pathway are substrates for ERK. Phosphorylation of Tsc1, Tsc2, and mTORC1 by ERK has been shown to increase mTORC1 activity. ERK also phosphorylates GAB (Grb2-assiciated binding protein) providing cross-inhibition, limiting mTOR signaling. Likewise, PI3K signaling acts through AKT to down regulate ERK activity through the phosphorylation and subsequent inactivation of Raf. Positive crosstalk is also present as multiple members of the Ras pathway have been shown to activate PI3K signaling, resulting in the combined effort of

ERK and mTOR signaling. This occurs at the top levels of each pathway as Ras activates PI3K (Kodaki *et al.* 1994) as well as downstream where both ERK and RSK are able to release Tsc1/2 repression of mTOR while simultaneously activating mTORC1 through the phosphorylation of Raptor (Carriere *et al.* 2011).

The importance of Ras/Raf/MEK/ERK signaling in gametogenesis

Interaction between the germ cell and the soma is of critical importance for the proper development of the sperm and egg alike. The Glial cell-derived neurotrophic factor (GDNF) is one of the most important signaling proteins for the maintenance of spermatogonial stem cell self-renewal and differentiation and has been shown to act through the Ras/Raf/MEK/ERK pathway (He *et al.* 2008). As GDNF binds to Ret, Grb2 is recruited activating Ras signaling and promoting cell cycle progression in the SSC. This increase in cell proliferation caused by GDNF can be blocked through the use of the ERK inhibitor PD98059 (He *et al.* 2008).

Kit ligand also serves as a necessary signaling molecule for spermatogenesis (Zhang *et al.* 2011). Produced by the Sertoli cell, Kit ligand binds to the Kit receptor and activates both the Ras/Raf/MEK/ERK and the PI3K/PKB/mTOR signaling pathways. Ectopic expression of an activated Kit allele harboring the D814Y mutation resulted in abnormalities in sperm morphogenesis (Schnabel *et al.* 2005). Kit also plays a necessary role in ovarian follicle maturation (Bedell *et al.* 1995). However, Kit signaling has been shown to be dispensable for primordial follicle activation, at least via the PI3K pathway (John *et al.* 2009).

N-Ras in particular is the predominant Ras isoform of the mouse testis. The high expression level of *N-Ras* in the testis is in fact greater than all other isoforms in all other tissues observed (Leon *et al.* 1987). N-Ras expression during spermatogenesis is detected

in undifferentiated spermatogonia and persists through the leptotene and zygotene stages of meiosis.

The function of the Ras family members has also been extensively studied in the context of Xenopus oocyte maturation. Xenopus oocytes become naturally arrested in prophase of meiosis I; however, this arrest can be removed through exposure to insulin, progesterone, and a number of other growth factors. Injections of purified Ras proteins have been able to activate the oocyte maturation (Birchmeier *et al.* 1985). Conversely, insulin-dependent maturation can be blocked through the injections of antibodies against Ras as well as multiple downstream members of the signaling pathway (Liang *et al.* 2007). This effect of Ras mutants on the mitosis to meiosis in oocytes has, to this point, not been investigated in the context of spermatogenesis.

Dissertation objective

Prior to the studies described in this dissertation, the role of *Rheb* and *N-Ras* in gametogenesis had not been described. *Tsc1* and *Tsc2* had been shown to be required for the regulation of primordial follicle activation. Since the only known function of the Tsc1/2 complex is to inhibit mTOR signaling via Rheb, Rheb presented as an interesting candidate to study. Additionally, crosstalk between the Ras/Raf/MEK/ERK and PI3K/PKB/mTOR signaling pathway had been described in the context of multiple cancers; however, the effect of these interactions had not been characterized in the gonad. Utilizing conditional genetic approaches, I studied the role of *Rheb* and *N-Ras* in both the male and female germ cell, employing a floxed allele of *Rheb* and a conditionally-active allele of *N-Ras*. These analyses revealed distinct defects in spermatogenesis in both conditional mutants generated, while oogenesis remained unaffected. An in-depth characterization of each phenotype determined the precise stage of spermatogenesis affected however further investigation will be required for the identification of a molecular mechanism. These studies are the first in vivo experiments demonstrating an essential role for *Rheb* and *N-Ras* in spermatogenesis. The primary focus of this dissertation discusses the defective meiotic progression and spermiogenesis phenotypes observed upon germ cell loss of *Rheb* and *N-Ras*.

Additionally, I employed gene expression profiling of neonatal ovaries to identify the genes regulating primordial follicle activation. My initial strategy was to focus on genes differentially expressed as a result of loss of the transcription factor Foxo3 which has been clearly defined as a molecular switch repressing PFA while in the active nuclear localized state. While remarkably few genes were deregulated in PD3 *Vasa-Cre; Foxo3*$^{L/-}$ compared to *Vasa-Cre* negative controls, I was able to identify the genes differentially expressed between PD1, PD3, PD7 and PD14 wild-type ovaries. These lists of genes will further multiple lines of questioning including interests in cell surface

receptors important to follicle development as well as downstream targets of the Foxo3 transcription factor regulating PFA. All in all, this dissertation provides the first account of an essential role in spermatogenesis for both *Rheb* and *N-Ras*, and further elucidates the extent to which the PI3K/PKB/mTOR and Ras/Raf/MEK/ERK signaling pathways regulate gametogenesis.

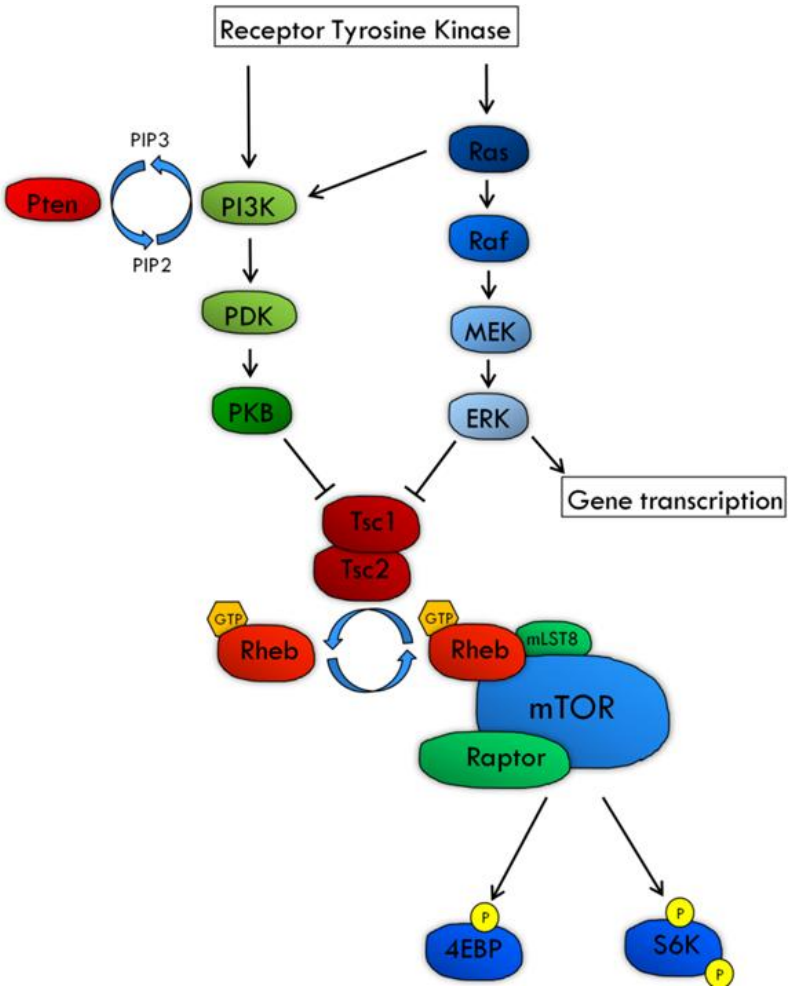

Figure 2.1) Overview of the PI3K/PKB/mTOR and Ras/Raf/MEK/ERK signaling pathways. This figure illustrates the canonical interaction of the core pathway members as well as the major points of interaction between the two pathways. As the activated receptor tyrosine kinase signals through PI3K or Ras, either downstream kinase cascade is activated, ultimately leading to the shared regulation of important biological processes including cell proliferation and metabolism. Negative feedback regulation is not shown for simplicity.

CHAPTER THREE

Methodology

Mouse strains, breeding, and tissue processing

This study was approved by the University of Texas Southwestern Medical Center Institutional Animal Care and Use Committee. Generation of both the *Rheb* floxed and *Vasa-Cre* alleles and genotyping protocols were previously described (Gallardo *et al.* 2007, Zou *et al.* 2011). *Vasa-Cre* males were crossed with $Rheb^{f/f}$ females. *Vasa-Cre*; $Rheb^{f/+}$ male offspring were again crossed to $Rheb^{f/f}$ females to produce *Vasa-Cre*; $Rheb^{f/-}$ experimental mice. Matched *Vasa-Cre* negative siblings were used as controls. All tissues were processed immediately after procurement. Tissues were fixed in 10% neutral buffered formalin for 24 hours, embedded in paraffin, and cut into 5-microns sections for immunohistochemistry (IHC) or H&E staining. Tissue sections from experimental and control samples were placed on the same slide to ensure identical processing.

Sperm analysis and breeding assays

A complete sperm analysis was performed to quantify the output of the testis. Epididymal sperm density was obtained by counting the number of hematoxylin-stained sperm heads in three 20x fields for each epididymis. The area in the seminiferous tubule was calculated using the ImageJ software package (Schneider *et al.* 2012). Data was graphed as total sperm per square pixel. Epididymal sperm concentration was used as a secondary measure of total sperm output. One epididymis was dissected and placed into one ml of phosphate buffered solution. Approximately 5 cuts were made in the epididymis followed by thirty minute incubation at 37˚C to release the sperm from the

tissue. Sperm concentration was then measured using a fixed cover slip counting chamber (Cell-Vu, DRM-600). Motility was also noted but experimental samples contained too few sperm for percentages to be accurately calculated. To study sperm morphology, a small drop of the sperm suspension was placed on a glass microscope slide and was spread evenly across the slid with a cover slip. The sperm smear was allowed to dry and was then subjected to Diff-Quik staining (Harleco, 65044C). Previously published criteria were used for the determination of normal sperm morphology (Wyrobek & Bruce 1975). Breeding assays were performed as previously described (Gallardo *et al.* 2008). Three week-old experimental and sibling control males were placed with two six week-old FVB females and observed for 20 weeks. Females were placed with one FVB male and observed for 18 weeks.

Immunohistochemistry and quantitative analyses of morphology in tissue sections

Slides were deparaffinized in xylene, hydrated in an ethanol series, subjected to antigen retrieval by boiling in 10 mM sodium citrate (pH 6.0) for 15 min, and cooled at room temperature (RT) for 20 min. After peroxidase blocking (3% hydrogen peroxide in water) for 30 min, slides were washed in water and then blocked in bovine serum albumin (BSA, 1% in 1x PBS) for 15 min. Slides were then incubated with primary antibody overnight at 4˚C, subjected to a TBST (1 M Tris-HCL, 5 M NaCl, 1x Tween-20) wash series, incubated with secondary antibody for 30 min at RT (Immpress; Vector Laboratories), and subjected to a second TBST wash series. Signal was detected using a DAB liquid chromogen substrate kit (DAKO). Slides were then counterstained with hematoxylin, rinsed in water, and air-dried. Antibodies and titers used included Foxo1 (rabbit monoclonal; Cell Signaling Technology, #2880; 1:500), Crem1 (rabbit polyclonal; Santa Cruz Biotechnology, #SC-440; 1:1000), mTOR (rabbit monoclonal; Cell Signaling Technology, #2983; 1:1000), p-mTOR (rabbit monoclonal; Cell Signaling Technology,

#5536; 1:1000), p-4EBP (rabbit monoclonal; Cell Signaling Technology, #9455; 1:1000), p-S6K (rabbit monoclonal; Cell Signaling Technology, #9234; 1:1000), p-S6 (rabbit monoclonal; Cell Signaling Technology, #4857; 1:1000), p-H2AX (rabbit monoclonal; Cell Signaling Technology, #9718; 1:200,000), Ki67 (rabbit monoclonal; Thermo Scientific, #RM-9106-FO; 1:500), germ cell nuclear antigen (GCNA; 1:200 IHC) (courtesy of George Enders, University of Kansas). Cell counts were performed to quantify the four principal cellular stages of sperm development (spermatogonia, spermatocytes, round spermatids and elongated spermatids). Counts for undifferentiated spermatogonia and round spermatids were facilitated by immunostaining these cell types with Foxo1 and Crem1, respectively, as described in the text. Spermatocytes and elongated spermatids were identified and counted based on their distinct morphology in routinely stained histologic sections. For each cell type, a minimum of twenty tubules (staged from IV to VII) were counted per mouse.

Tissue Homogenates and Cell Lysates

Previously frozen tissues were weighed and then mechanically homogenized on ice. The lysis buffer consisted of RIPA buffer (Thermo Scientific), cOmplete Mini EDTA-free protease inhibitor cocktail (Roche Diagnostics), and Phosphatase Inhibitor Cocktail 2 (Sigma-Aldrich). Following homogenization, suspensions were centrifuged at 13,000 rpm for 10 minutes in a microcentrifuge. The resulting supernatants were then divided into aliquots for protein quantification using a BCA protein assay kit (Pierce Biotechnology) and frozen storage at -20°C.

Western Blotting

Tissue homogenates (testis and ovary) were combined with an equal volume of Laemmli buffer (Bio-Rad Laboratories), boiled for 10 minutes, subjected to

SDS-polyacrylamide gel electrophoresis (Mini-PROTEAN TGX 12% Precast Gels, Bio-Rad Laboratories, 130 volts until migration complete), and transferred to polyvinylidene difluoride membranes (Immobilon-P, Millipore, 100 volts for 1 hour). Nonspecific antibody binding was blocked by incubation with TBST plus nonfat milk (5% in TBST) for one hour at RT. Membranes were then incubated with primary antibody overnight at 4˚C. After a TBST wash series, membranes were incubated with HRP-linked secondary antibody raised in donkey (ECL, GE Healthcare) for 1 hour at RT and then subjected to a second TBST wash series. Signal was detected using the SuperSignal West Dura chemiluminescent substrate detection kit (Thermo Scientific).

PAS-Feulgen staining

PAS-Feulgen staining was performed to visualize the formation of the acrosome. Slides were submitted to the UT Southwestern histology core and processed using standard protocols.

TUNEL assay

ApoTag Peroxidase *In Situ* Apoptosis Detection Kit was used according to manufacturer's instructions. Chromogenic substrate (DAKO) was for detection of the immunoperoxidase bound to the fractured DNA of apoptotic cells. Controls were placed on the same slide to ensure identical processing.

Expression profiling

Testes were dissected from PD3 mice and immediately homogenized in 0.5 ml Tripure (Roche). RNA was prepared per the manufacturer's instructions and resuspended in RNase-free water (14 µl/ovaries). Quality and purity of the RNA was checked by spectrophotometry and gel electrophoresis. RNA samples were submitted to the UTSW

Microarray Core for labeling and hybridization per standard protocols. Each genotype was submitted in triplicate using independent testis samples and hybridized to the Illumina Mouse-6 V2 BeadChip. Analysis was performed using BeadStudio software with quantile normalization.

Statistics

Data were graphed and analyzed using GraphPad Prism 5. Two-tailed Student's *t* tests were used to evaluate significance and calculate *P* values, with threshold values as described in the results or figure legends. Error bars represent standard error of mean values. A *P* value of less than 0.05 was considered significant.

Table 3.1: PCR primers and conditions for genotyping*

Gene	Primers 5'-3'	Annealing Temp (˚C)	Products (bp)
Vasa-Cre	CACGTGCAGCCGTTTAAGCCGCGT TTCCCATTCTAAACAACACCCTGAA	55	(+) 240
Rheb	GCTGTCAGATCCACTGCAAG GCCCAGAACATCTGTTCCAT ATAGCTGGAGCCACCAACAC GCCTCAGCTTCTCAAGCAAC	55	(+) 650 (F) 850 (–) 650
N-Ras Q61R-LSL	GCAAGAGGCCCGGCAGTACCTA AGACGCGGAGACTTGGCGAGC GCTGGATCGTCAAGGCGCTTTTCC	62	(+) 487 (LSL) 371
Foxo3	AACAACCTCACACATGTGCC AGTGTCTGATACCGAAGAGC CATGCAGTCCGAGAGATTTG	55	(+) 170 (F) 208 (–) 246
Tsc1	AGGAGGCCTCTTCTGCTACC CAGCTCCGACCATGAAGTG AGCCGGCTAACGTTAACAAC	58	(+) 295 (F) 235
Pten	AAGCACTCTGCGAACTGAGC TTGCCAGACATGCTCCGAAG GCTTGATATCGAATTCCTGCAGC	58	(+) 400 (F) 650 (–) 370
Rosa26	AAAGTCGCTCTGAGTTGTTAT GCGAAGAGTTTGTCCTCAACC GGAGCGGGAGAAATGGATATG	65	(+) 680 (LSL) 350

*All genotyping PCR reactions were performed using Promega GoTaq polymerase (#3001) and reagents.

Programs were 95°C 2min; 94°C 30sec, Annealing Temp 30sec, 72°C 30sec (35 cycles); 72°C 7min.

CHAPTER FOUR

Results

THE SMALL GTPASE RHEB IS REQUIRED FOR SPERMATOGENESIS BUT NOT OOGENESIS

Conditional inactivation of Rheb in the germline with Vasa-Cre

A floxed *Rheb* allele (*Rheb*^{f}) was crossed with the germ cell specific Cre recombinase, *Vasa-Cre*. This strategy allows for prenatal deletion of *Rheb* in both the male and female germlines, as *Vasa-Cre* is expressed in both male and female germ cells beginning at embryonic day 15 (E15) (Gallardo *et al.* 2007). Confirmation of *Vasa-Cre* mediated excision of the floxed third exon of the *Rheb* locus was performed through PCR genotyping of both the *Rheb* floxed and *Rheb*-null alleles in *Vasa-Cre; Rheb*$^{f/+}$ mice. Both the wild-type and floxed *Rheb* alleles were detected in multiple tissues of *Vasa-Cre; Rheb*$^{f/+}$ mice, however, the floxed allele was clearly less abundant in the testis, consistent with germ cell Cre recombination and *Rheb* inactivation (**Fig. 4.1A**). The *Rheb*-null allele was detected in the testis of the *Vasa-Cre; Rheb*$^{f/+}$ mouse but not in other tissues (**Fig. 4.1B**) again consistent with germ cell specific Cre activity. Germline transmission of the *Rheb*-null allele was also confirmed by genotyping progeny from *Vasa-Cre; Rheb*$^{f/-}$ females crossed to wild-type males; all progeny carried the *Rheb*-null allele (n=18), confirming efficient, biallelic ablation of *Rheb* within oocytes.

Gross and histological analyses of gonads from male and female Rheb conditional knockout (cKO) mice

By gross examination, adult *Rheb* cKO (*Vasa-Cre; Rheb*$^{f/-}$) testes were much smaller than those of *Vasa-Cre* negative (*Rheb*$^{f/-}$) sibling controls (**Fig. 4.2A**). A progressive atrophy of the testes was observed in experimental males. *Vasa-Cre; Rheb*$^{f/-}$ testis weights underwent a further two-fold decrease in weight from three to five months of age (**Fig. 4.2B**). Testis sections from three month old *Vasa-Cre; Rheb*$^{f/-}$ males exhibited hypospermatogenesis with all stages of sperm present. However, in aged mice the seminiferous tubules were more severely affected by the loss of *Rheb*. At five months of age, there was severely decreased spermatogenesis and while spermatocytes were present, very few round or elongated spermatids were observed (**Fig. 4.2C**). In contrast, *Vasa-Cre; Rheb*$^{f/-}$ ovaries were grossly unremarkable (**Fig. 4.3A**). Histological analysis of ovary sections showed the presence of growing follicles of all stages (**Fig. 4.3B**) and a healthy pool of quiescent primordial follicles (**Fig. 4.3C**).

Rheb cKO males have decreased sperm counts and abnormal sperm morphology

A complete sperm workup was performed to identify defects in total sperm count, morphology and motility. Epididymides from both *Vasa-Cre; Rheb*$^{f/-}$ and *Rheb*$^{f/-}$ controls were examined histologicaly for the presence of mature spermatozoa (**Fig. 4.4A**). Quantification of sperm head density clearly showed a progressive age-dependent decrease of sperm production (**Fig. 4.4B**). This decrease was also quantified through epididymal sperm concentration counts (**Fig. 4.4C**). By four months of age the *Vasa-Cre; Rheb*$^{f/-}$ males exhibited severe oligoasthenoteratozoospermia. The predominant morphological defect observed was amorphous head shapes (**Fig. 4.4D**).

Rheb is required for male, but not female, fertility

To quantify the effect of *Rheb* cKO on fertility, breeding assays were set up for *Vasa-Cre; Rheb*$^{f/-}$ males and females and *Rheb*$^{f/-}$ sibling controls. The *Rheb* cKO female mice were fertile; their fecundity was indistinguishable from controls and they continued to have litters of normal size up to eighteen weeks of age (**Fig. 4.5A, B**). The male *Rheb* cKO mice, however, did not produce any offspring over a period of twenty weeks (**Fig. 4.5C, D**). This complete male infertility is expected given the previously defined oligoasthenoteratozoospermia.

Histological analyses of gametogenesis expose a defect in meiotic progression

As an initial characterization of the disrupted seminiferous tubules, and to identify potential developmental blocks in spermatogenesis, cell counts were performed to quantify numbers of spermatogonia, spermatocytes, round spermatids and elongated spermatids (**Fig. 4.6A**). Foxo1 expression was used as a convenient marker of undifferentiated spermatogonia (Goertz *et al.* 2011, Tarnawa *et al.* 2013). Immunostaining and counts revealed normal numbers of undifferentiated spermatogonia in *Vasa-Cre; Rheb*$^{f/-}$ testes at all time points (**Fig. 4.6C**). Spermatocytes were counted based on their large size and distinctive cellular morphology. A significant accumulation of spermatocyte was observed at two months but numbers reverted to normal at three and four month time points. By five months of age, a significant decrease in spermatocyte numbers was observed (**Fig. 4.6D**). Quantifications of round and elongated spermatids were performed through Crem1 immunostaining and cellular morphology, respectively (Delmas *et al.* 1993) (**Fig. 4.6B**). Decreases in round and elongated spermatid counts were observed at early time points (**Fig. 4.6C and 4.6D**). Thus in summary, *Rheb* cKO

males exhibited a striking age-dependent decrease in spermatid production and a more modest decrease in spermatocytes, while maintaining normal numbers of undifferentiated spermatogonia. These results point to abnormalities in meiotic progression.

Spermatogonia continue to proliferate and initiate meiosis

In light of the progressive decrease in spermatocytes in the *Vasa-Cre; Rheb*$^{f/-}$ mice, proliferation and meiotic entry were further evaluated by immunostaining for Ki67 and pH2AX, respectively. Ki67 is a marker of actively cycling cells, while H2AX is phosphorylated in response to double-stranded DNA breaks (Hamer *et al.* 2002, Akbay *et al.* 2013). Phosphorylated H2AX (pH2AX) nuclear foci serve as a marker of meiotic recombination in response to the formation of chiasma between sister chromatids in leptotene spermatocytes. However, detailed counts of cells positive for Ki67 and pH2AX foci revealed no significant differences between *Vasa-Cre; Rheb*$^{f/-}$ and control males at all time points studied (**Fig. 4.7**). Therefore, spermatogonial proliferation and meiotic entry *per se* appears largely unaffected in *Rheb* cKO males, again consistent with a severe defect in meitoic progression.

The activation state of mTOR, S6K and 4EBP appears to be unaffected

I then sought to determine the activation status of mTOR pathway components in *Rheb* cKO testes as well as ovaries. Immunohistochemistry was performed for phosphorylated (i.e. activated) mTOR pathway members p-mTOR, p-S6K, p-S6 and p-4EBP using well-validated phosphorylation site-specific antibodies for each of these factors. However, no significant differences were observed in the phosphorylation state

of any of these mTOR pathway components in *Rheb* cKO vs. control testes as gauged by staining intensity when specific spermatogenic stages were compared (**Fig. 4.8**).

RhebL1 may serve a functionally redundant role in the absence of Rheb.

Analysis of unpublished gene expression data gathered by the Castrillon lab reveals that *Rheb* is highly expressed in SSC culture and type A spermatogonia. Expression of *Rheb* then decreases in type B as the spermatogonia prepares for meiosis. *Rheb* is also highly expressed throughout ovarian development with greatest expression in the PD7 ovary (**Fig 4.9**). The *Rheb* homolog, *RhebL1*, closely mimics the expression pattern in the testis and is also expressed in the ovary, peaking at PD3 during primordial follicle assembly (**Fig 4.10**). Given the importance of gamete formation, extensive redundancies would provide much needed resilience against genetic mutations. This would explain the lack of phenotype in the female and could lead to insights into the age-dependence of the male phenotype.

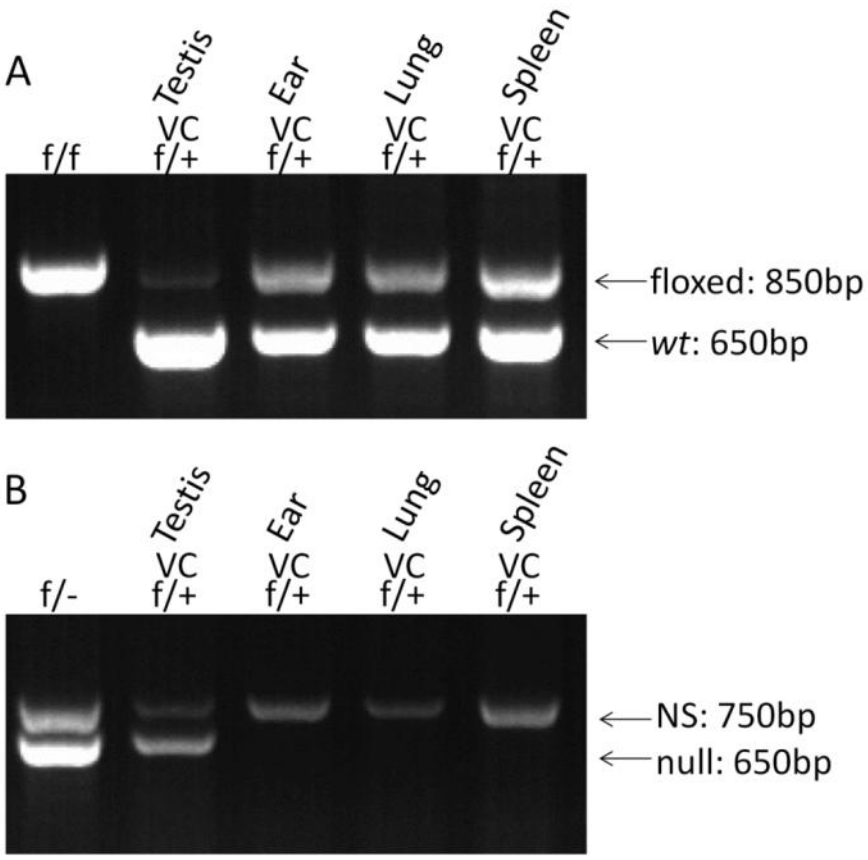

Figure 4.1) Genotype confirmation of germ cell *Rheb* conditional knockout. (A) An ethidium bromide-stained 1% agarose gel shows the presence of the *Rheb*-floxed allele (850 bp) in tail DNA from a *Rheb* homozygous floxed mouse as well as all tissues of a *Vasa-Cre; Rheb*$^{f/+}$ (heterozygous) male. The floxed (f) band is decreased in the *Vasa-Cre; Rheb*$^{f/+}$ testis consistent with *Vasa-Cre* mediated recombination in germ cells. The *wt* (+) band (650bp) is observed in tissues from this heterozygous male mouse, as expected. (B) Cre-mediated excision was further confirmed by the presence of the *Rheb* null allele (650bp) in a *Vasa-Cre*; *Rheb*$^{f/+}$ testis as well as a *Rheb*$^{f/-}$ control testis. The *Rheb* null allele was not detected in other tissues (e.g. skin, lung, and spleen). NS = non-specific PCR product (~750bp).

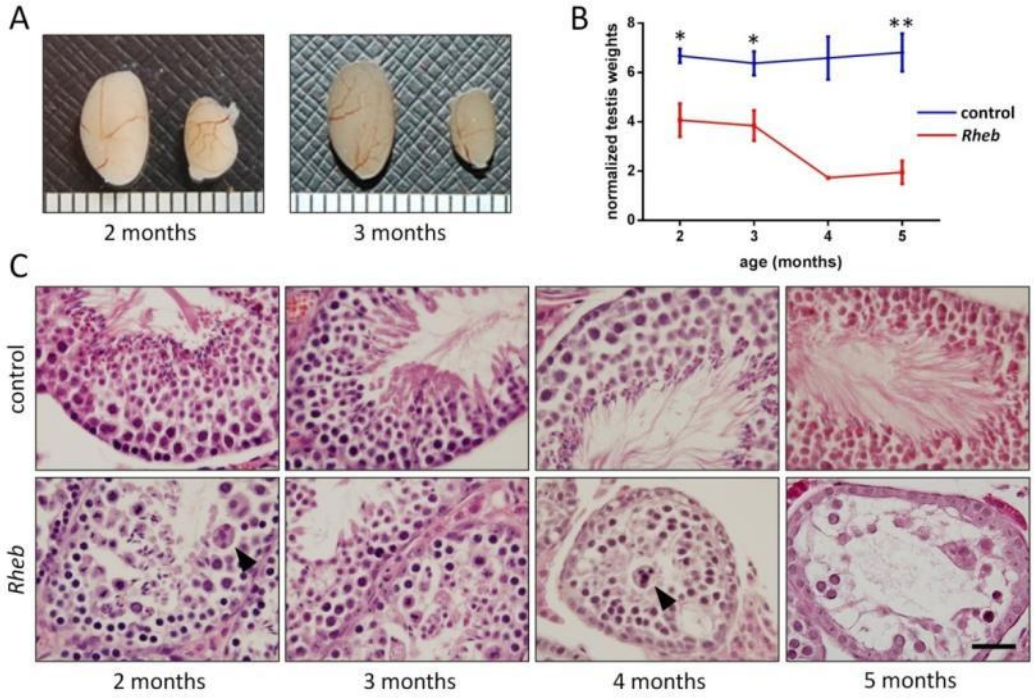

Figure 4.2) Conditional *Rheb* inactivation results in a progressive defective of spermatogenesis. (A) Intact testes. Right = *Vasa-Cre; Rheb*$^{f/-}$; Left = *Rheb*$^{f/-}$ sibling control. Ruler markings = 1 mm. (B) Testis weights in mice of different ages. Red = *Vasa-Cre; Rheb*$^{f/-}$; Blue = *Rheb*$^{f/-}$ sibling control. **P* < 0.05, ***P* < 0.005, by unpaired T test (two months, n = 2; three months, n = 3; four months, n = 1; five months, n = 3) (C) H&E stained tissue sections from testes of two to five month-old *Rheb* cKO and sibling control mice. Representative fields illustrate an abnormal organization of seminiferous tubules at the two month time point and the age-dependent defect in meiotic progression resulting in the progressive loss of round and elongating spermatids in the 5 month-old testis. Arrowheads indicate large multinucleated germ cells. Bar = 50 microns.

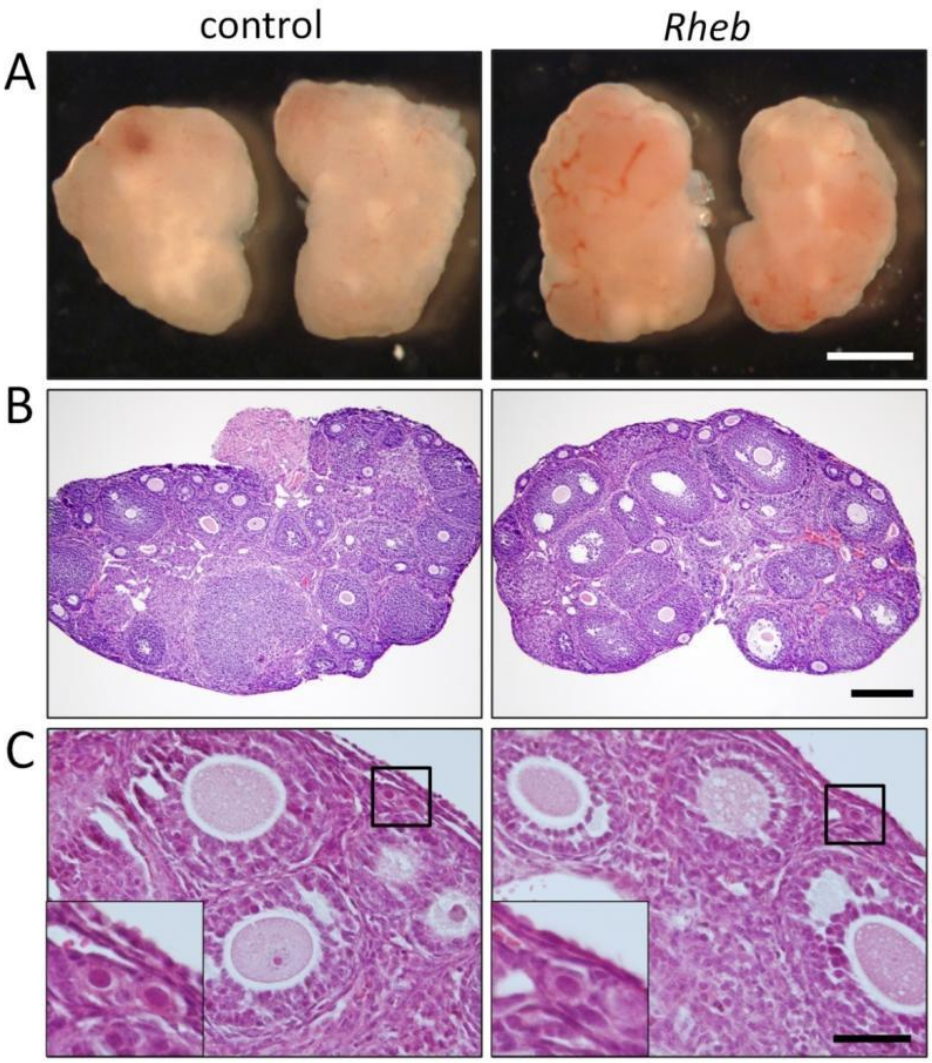

Figure 4.3) Ovaries of *Rheb* cKO mice are grossly normal and contain growing follicles of all stages as well as morphologically-normal primordial follicles. (A) Intact ovaries of *Rheb* cKO females were of similar size and shape relative to sibling controls. Bar = 1 mm. (B) H&E stained tissue sections from experimental and control ovaries revealed growing follicles of all stages. Bar = 250 microns. (C) Higher magnification shows growing primary and secondary follicles. Insets: morphologically normal, quiescent, primordial follicles. Scale bar = 50 microns.

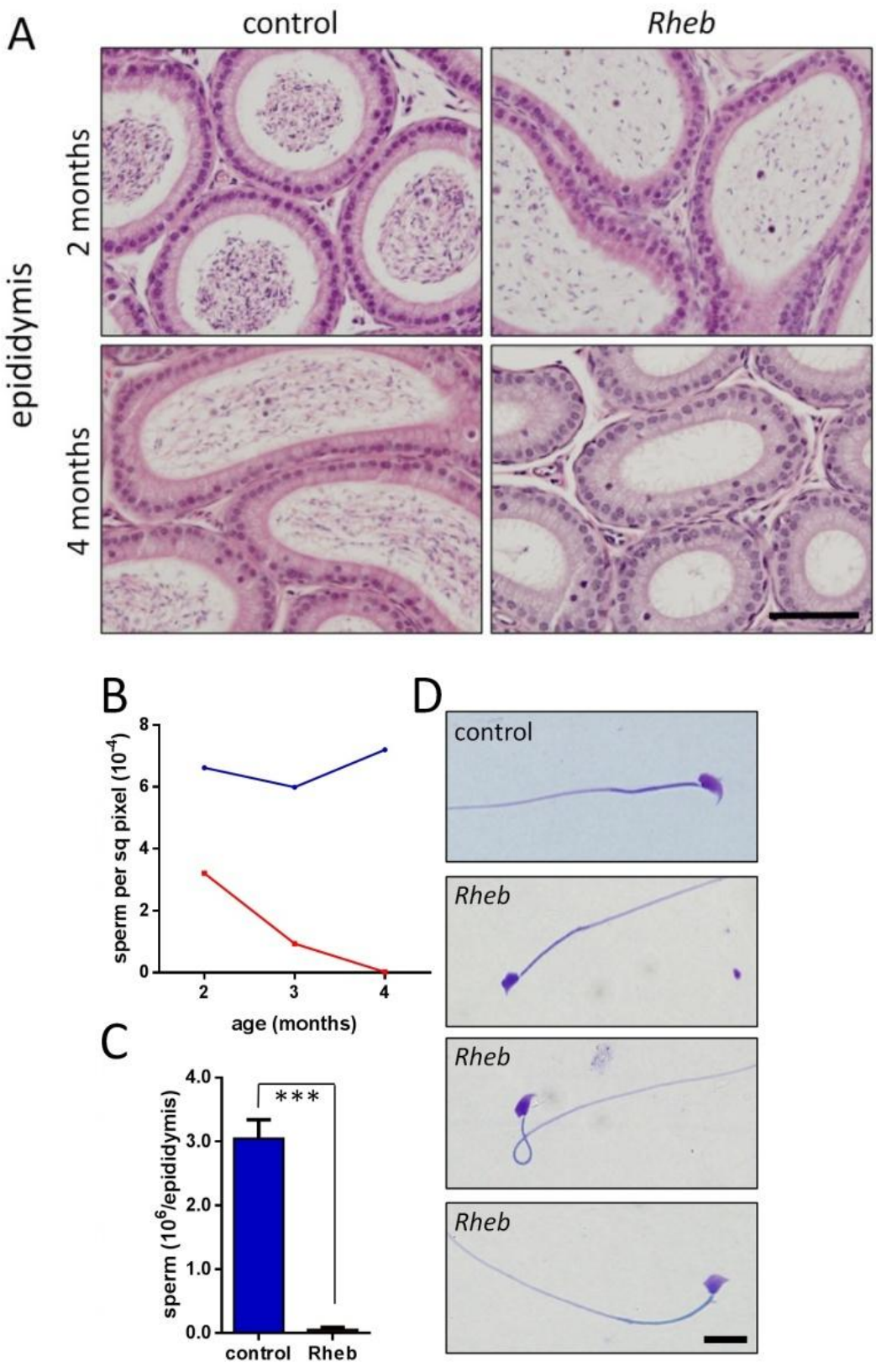
A
control
Rheb
epididymis
2 months
4 months
B
sperm per sq pixel (10^{-4})
8
6
4
2
0
2
3
4
age (months)
C
sperm (10^6/epididymis)
4.0
3.0
2.0
1.0
0.0
***
control
Rheb
D
control
Rheb
Rheb
Rheb

Figure 4.4) Total sperm production is drastically decreased and remaining sperm are malformed. (A) Histology of epididymides from control and experimental mice. Bar = 100 microns. (B) The decrease in epididymal sperm was quantified by sperm head density counts (n = 1 for all time points and genotypes). (C) Total sperm counts were performed after releasing the sperm from the epididymis. ***$P < 0.0001$. Red = *Vasa-Cre; Rheb*$^{f/-}$ n = 4; Blue = *Rheb*$^{f/-}$ n = 5 sibling control. (D) The few sperm obtained from the epididymis of *Rheb* cKO mice were all immotile and exhibited abnormal morphology. Bar = 10 microns; all panels at same magnification.

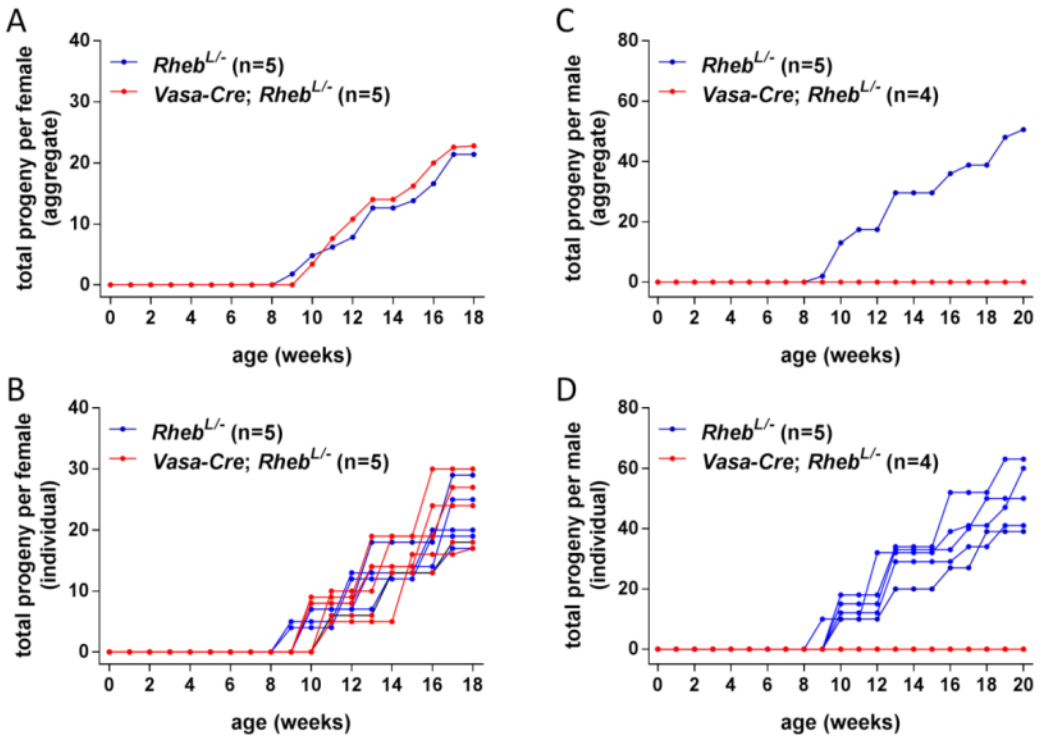

Figure 4.5) Serial breeding assays reveal that *Rheb* cKO males are sterile while *Rheb* cKO females are fertile with normal fecundity to 18 weeks of age. (A) Aggregate (i.e. all animals of the same genotype averaged) and (B) Individual (i.e. every line represents a single animal) representations of total progeny per female. (B) Aggregate and (C) Individual representations of total progeny per male.

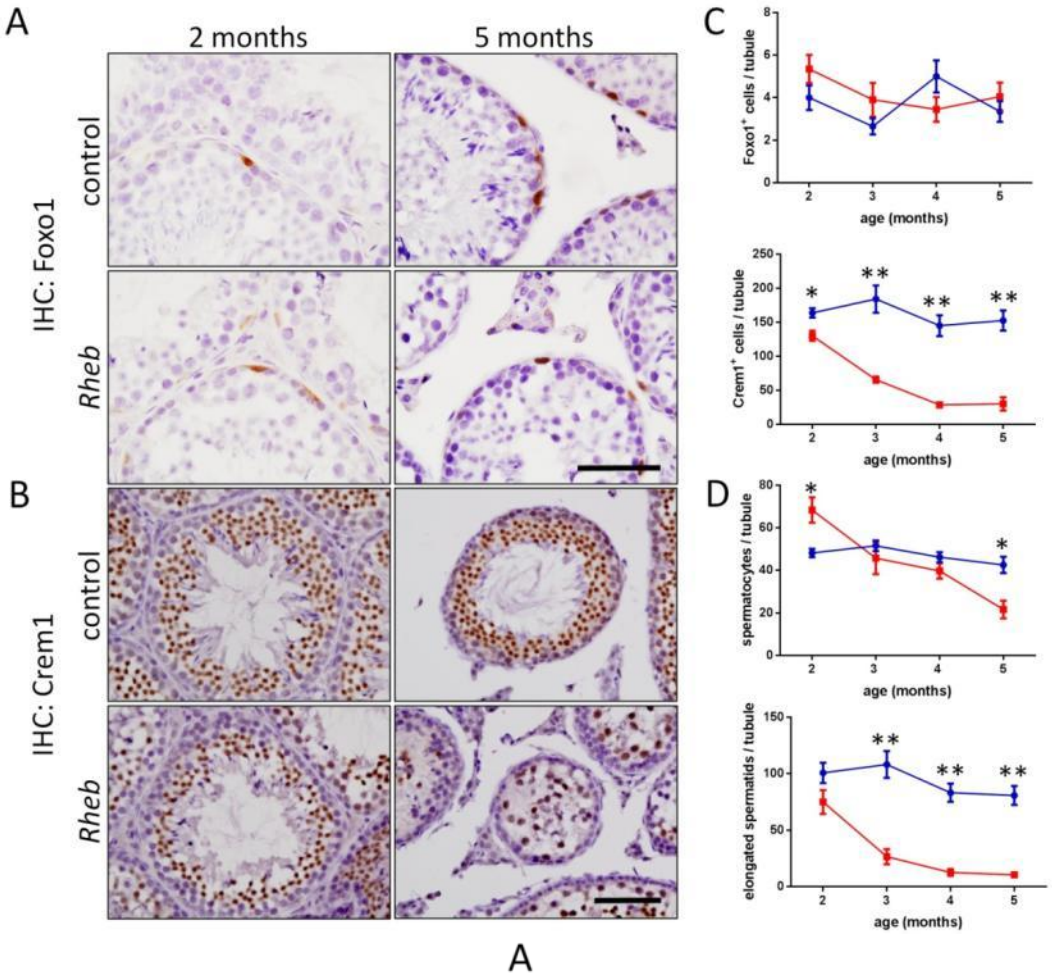

Figure 4.6) Cell counts reveal meiotic progression defect. (A) Foxo1 and (B) Crem1 immunostains of experimental and control testes at two and five months of age. Bar = 50 microns and 100 microns, respectively. (C) Quantification of Foxo1 and Crem1 positive cell counts in twenty tubules; **P* < .05, ***P* < 0.0005 by unpaired T test. (D) Counts of spermatocytes and spermatids in hematoxylin-stained tissue sections. The counts of elongated spermatids closely mirrored the observed decrease in $Crem1^{+}$ round spermatids; **P* < 0.05, ***P* < 0.005, ****P* < 0.0005, by unpaired T test.

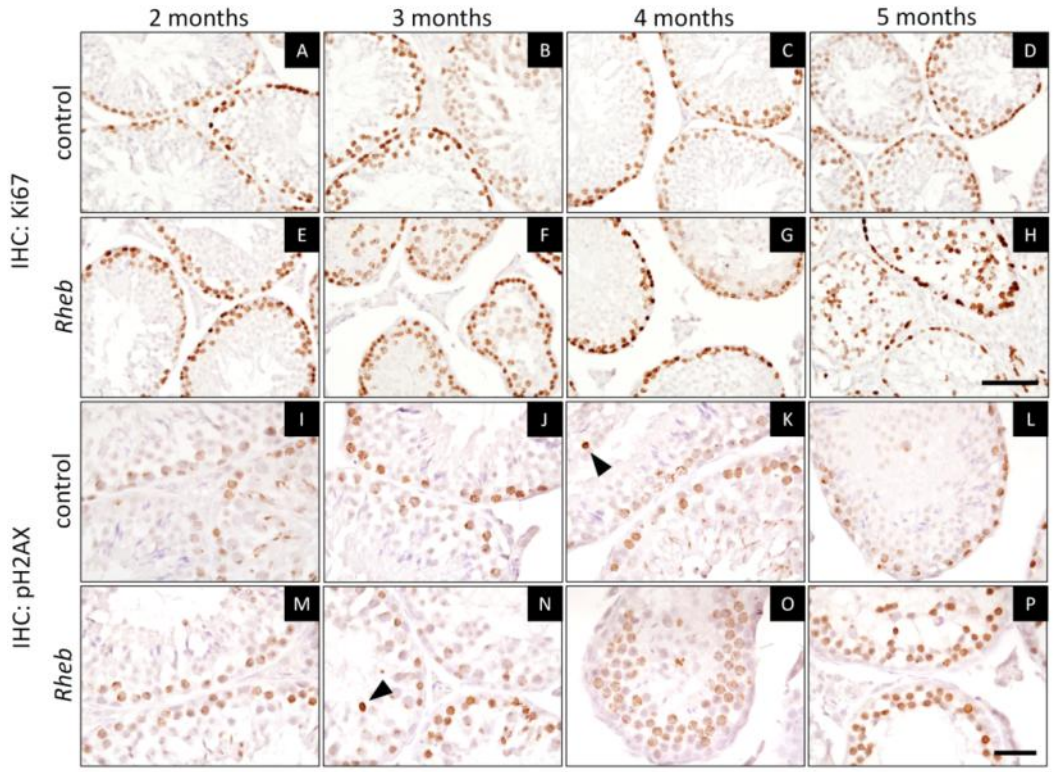

Figure 4.7) Analyses of cell proliferation and meiotic entry. (A-H) Immunostaining for Ki67 as a marker for cellular proliferation. Bar = 100 microns (I-P) Immunostaining for pH2AX as a marker of meiotic entry. Scattered apoptotic germ cells server as an internal positive control (arrowheads) since apoptotic cells undergo DNA fragmentation and are strongly positive for pH2AX. Bar = 25 microns.

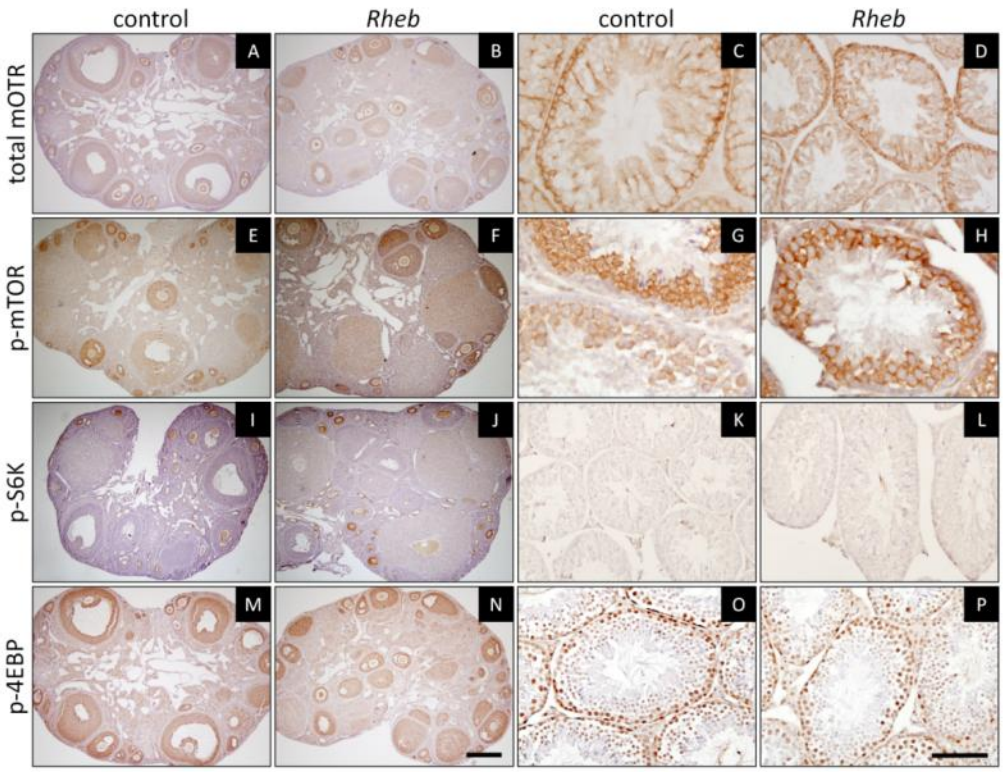

Figure 4.8) Analysis of mTOR and downstream effectors. Immunostains with phosphorylation-site specific antibodies against canonical mTOR pathway members in both ovaries (left) and testes (right). Bar = 250 microns and 100 microns, respectively. (A-D) Total mTOR. (E-H) p-mTOR. (I-L) p-S6K. (M-P) p-4EBP.

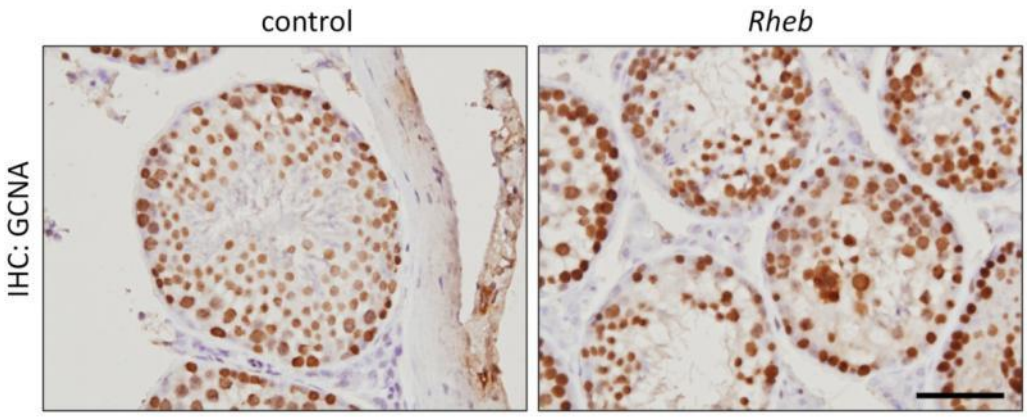

Figure 4.9) Cells remaining in seminiferous tubules express the germ cell marker GCNA. Immunostaining for the male germ cell marker GCNA in the testes of five month old *Rheb* cKO (*Vasa-Cre; Rheb*$^{f/-}$) and control testes. Bar = 50 microns.

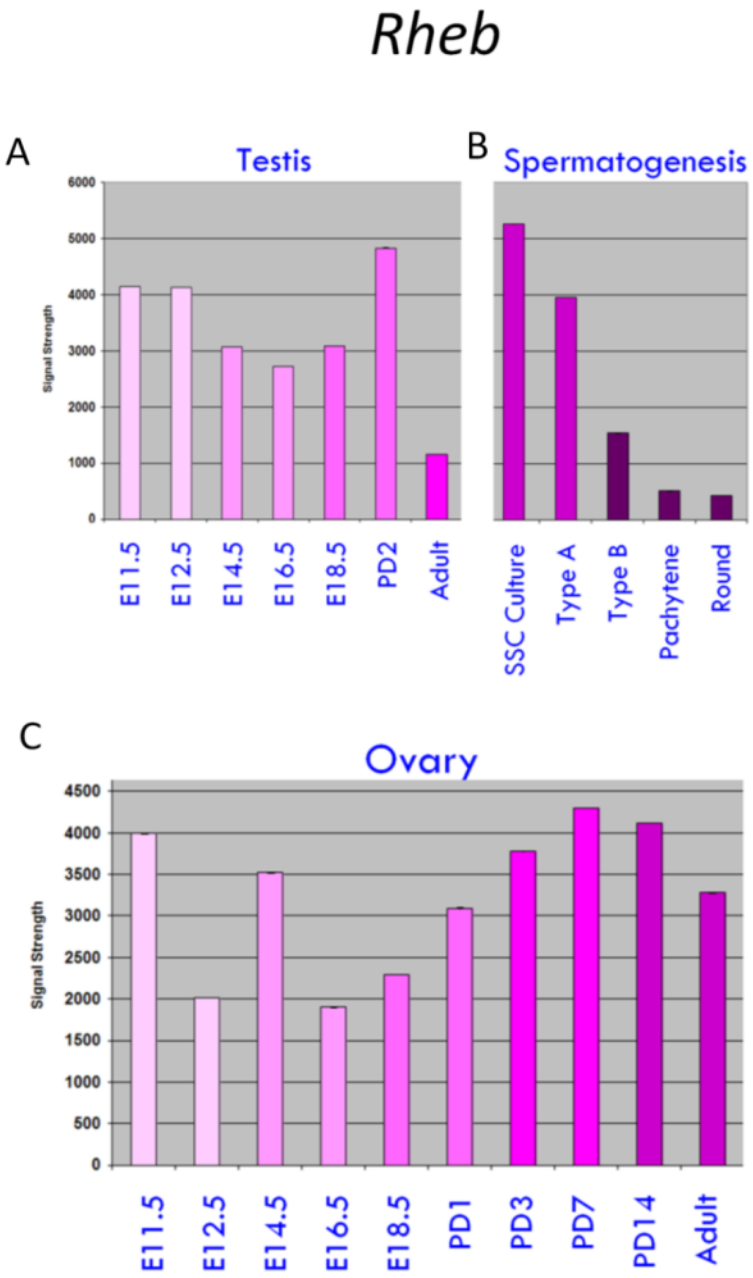

Figure 4.10) Changes in *Rheb* mRNA levels determined by gene expression microarray (Affymetrix 430 AB). Expression of *Rheb* across A) embryonic, neonatal and adult testes, B) spermatogenesis and C) embryonic, neonatal and adult ovaries.

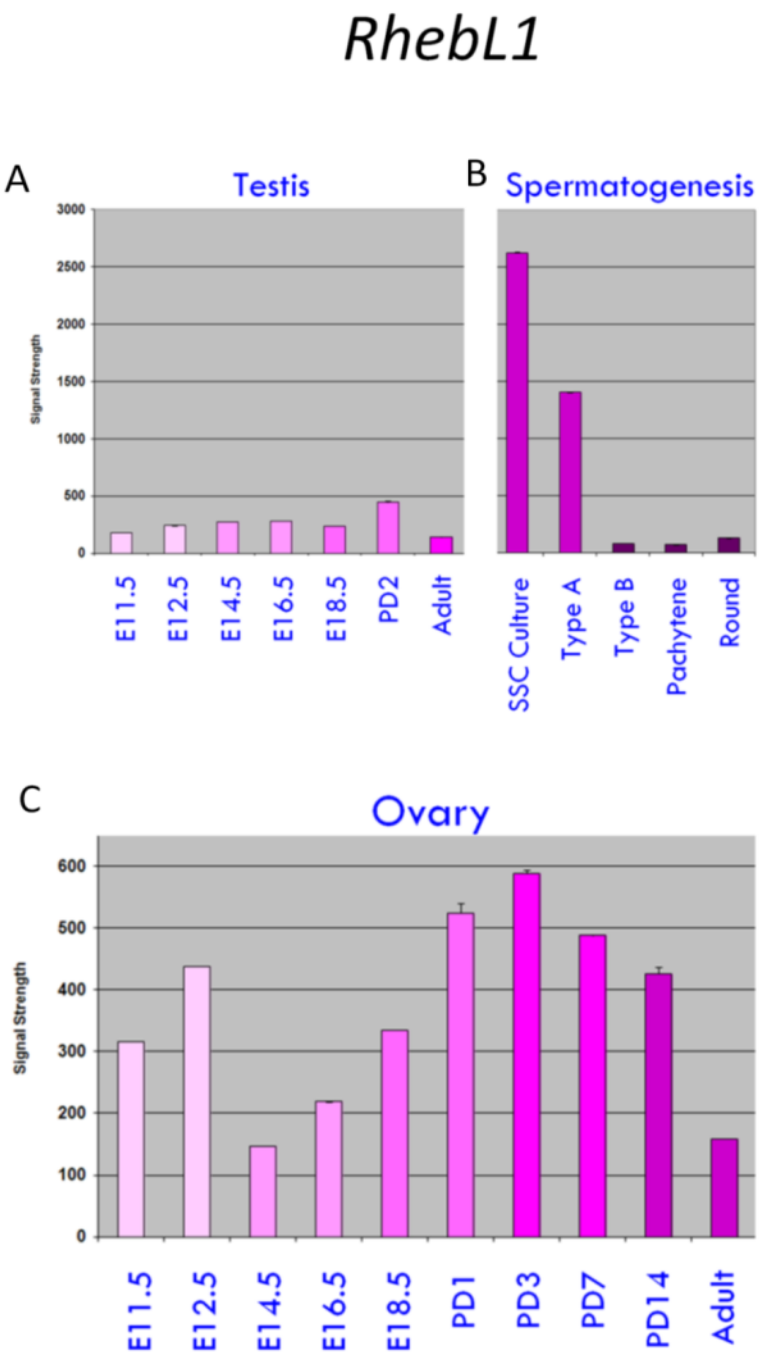

Figure 4.11) Changes in *RhebL1* mRNA levels determined by gene expression microarray. Expression of *RhebL1* across A) embryonic, neonatal and adult testes, B) spermatogenesis and C) embryonic, neonatal and adult ovaries.

CHAPTER 5

Results

CONSTITUTIVELY ACTIVE N-RAS DISRUPTS SPERMIOGENESIS

Introduction

Based on the previously established cross-talk between the Ras/Raf/MEK/ERK and the PI3K/AKT/mTOR signaling pathways it was hypothesized that these interactions could be exploited to further elucidate the regulation of primordial follicle activation. In this light, Ras presented as an interesting candidate for genetic studies in the ovary. Specifically, *N-Ras* was chosen as it is the predominantly expressed *Ras* in the ovary as well as in the testis (which expresses the highest levels of *N-Ras* than any other tissue observed) (Leon *et al.* 1987). *N-Ras* has also been shown to be expressed in mitotically active spermatogonia, persisting through prophase of meiosis suggesting a potential role in the mitosis to meiosis transition (Wolfes *et al.* 1989). Analysis of Castrillon lab gene expression profiles confirms both previous observation and further supports the claim that N-Ras plays an essential role in spermatogenesis (**Fig 5.1**). A constitutive activation strategy, utilizing the well-characterized Q61R mutation, was employed to force an increase in signal either directly through PI3K or through downstream activation of mTOR by ERK.

The *N-Ras Q61R* allele was constructed and generously provided by Christin Burd and Norman Sharpless from the University Of North Carolina School Of Medicine. The activating mutation was introduced in N-Ras protein converting a glutamine to an arginine. This mutation disrupts the catalytic site preventing the hydrolysis of GTP, locking N-Ras in the active state. The *N-Ras* activating mutations, including *Q61R* and *Q61K*, were discovered due to the major impact they have on the initiation and

progression of multiple cancer types, melanoma in particular. However, while present in testicular germ cell tumors (varying reports of 15-40%), it does not appear to be necessary or sufficient to drive germ cell tumors (Olie *et al.* 1995). The *N-Ras Q61R* allele includes a lox-stop-lox (LSL) cassette upstream of the *N-Ras* gene which under basal conditions prevents the expression of this mutant *N-Ras* allele. Once crossed with a Cre recombinase, the stop codon is excised and expression is driven by the endogenous (i.e. wild-type) *N-Ras* promoter.

Conditional constitutive activation of N-Ras in the germline with Vasa-CreERT2

Germ cell activation of the *N-Ras Q61R* allele was pursued to further elucidate the pathways controlling PFA. To study the effect of constitutive activation of N-Ras in the germ cell *Vasa-Cre* was again employed as our germ line specific Cre. This strategy, however, was unsuccessful as it was discovered that the cross of *N-Ras*^{LSL} heterozygote females to *Vasa-Cre* heterozygote males did not yield a single double positive pup out of seven litters (n = 51; expected n=12.8 by Mendellian ¼ ratio). This embryonic lethality of *Vasa-Cre* driven *N-Ras* activation is likely due to ectopic expression of *Vasa-Cre* in a rare cell type which was not observed in the initial characterization of the *Vasa-Cre* allele. Alternatively, hyper-proliferative embryonic germ cells could adversely affect embryo development, although this seems less likely.

An alternative strategy utilizing a tamoxifen (TAM) inducible *Vasa-CreERT2* strain provided experimental *Vasa-CreERT2; N-Ras*$^{LSL/+}$ (*N-Ras Q61R*) mice with expected Mendelian ratios. This inducible Cre was verified through the use of a *Rosa26* reporter strain (**Fig. 5.2**). Once exposed to TAM, the germ cell specific Cre turns on the Rosa26 beta-galactosidase reporter gene. After X-Gal staining, cells expressing the activated Cre

stained blue (**Fig 5.1**). Recombination of the *N-Ras*^{LSL} allele was confirmed through PCR genotyping of the floxed and activated allele. After induction of *Vasa-CreERT2* mediated recombination, mice were sacrificed and gonads were examined for defective gametogenesis after defined intervals.

Gross and histological analyses of gonads from Vasa-CreERT2; N-Ras$^{LSL/+}$ *mice reveals immature germ cells in the epididymis*

Testis weights, which often reveal early defects in spermatogenesis, were not significantly altered in *Vasa-CreERT2; N-Ras*$^{LSL/+}$ males vs. *N-Ras*$^{LSL/+}$ sibling controls (**Fig. 5.3**). However, upon histological investigation it was apparent that a severe defect in spermiogenesis was resulting in an increase of round spermatids which were not proceeding normally through elongation and maturation. Despite this severe block in elongation, spermiation appeared to be proceeding as the round spermatids were released into the lumen of the seminiferous tubule and transported to the epididymis (**Fig 5.4**). A similar phenotype (i.e. immature germ cells in the semen) has been observed in infertile men with apparent arrest of spermiogenesis (Caskurlu *et al.* 1999, Yeung *et al.* 2007).

Ovaries from *N-Ras Q61R* females were histologicaly normal, containing a healthy pool of primordial follicles, activated primary follicles as well as pre-ovulatory antral follicles (**Fig 5.5**). Breeding assays were not performed as the normal histologic appearance of the ovary argued against the likelihood of an infertility phenotype.

Immunostaining of undifferentiated spermatogonia and round spermatids

Immunostaining for Foxo1 allowed for quantification of the undifferentiated spermatogonia population which was not affected by the activated *N-Ras* allele (**Fig. 5.6**). Using Crem1 as a marker of round spermatids, detailed counts confirmed that the increase of round cells in the seminiferous tubule (**Fig 5.7**). Crem1 expression was also used to confirm the identity of the round cells populating the epididymis (**Fig. 5.8**)

Constitutively active N-Ras resulted in an increase in seminiferous tubules containing apoptotic cells

To determine if the round spermatids were undergoing apoptosis, TUNEL staining was performed. An increase in seminiferous tubules containing apoptotic germ cells was observed. While several tubules appeared to be undergoing dramatic apoptotic collapse (**Fig. 5.9**), most spermatids appeared to avoid apoptosis as they migrate to the epididymis. While the majority of immature spermatids manage to avoid apoptosis, they are still haploid cells and inherently unable to replicate, limiting any malignant potential resulting from the activation of *N-Ras* in the testis.

Round spermatids display normal acrosome biogenesis but defective elongation.

Periodic Acid-Schiff-positive (PAS)-Feulgen staining provides a method for observing acrosome formation in great detail by staining the poly-saccharide rich acrosomal vesicles a dark purple while staining the nucleus a deep pink. As the acrosomal vesicle forms, a dark point is visible on the anterior pole of the nuclear membrane. The acrosome vesicle then thins to form the acrosome cap. This process was

unaffected in *N-Ras Q61R* mice, however, elongation of the acrosome was not observed consistent with the hypothesis that the defect is occurring in the elongation phase of spermiogenesis (**Fig. 5.10**).

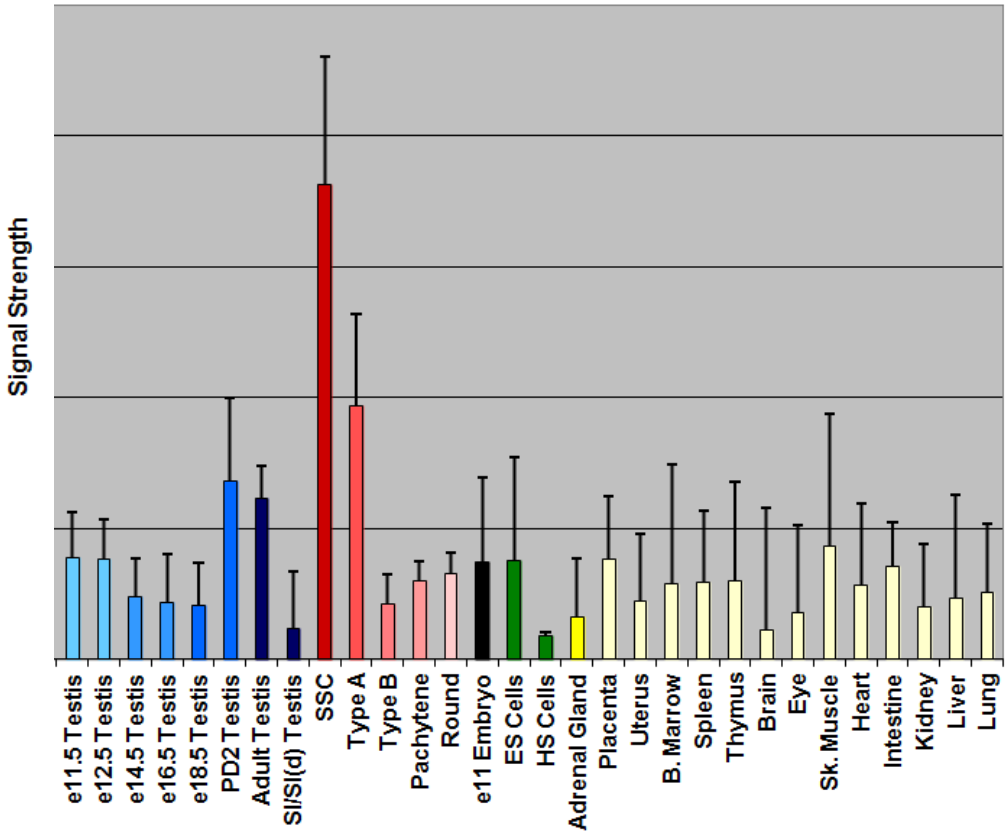

Figure 5.1) ***N-Ras*** **mRNA expression data implies an important role in spermatogenesis.** *N-Ras* is highly expressed in both neonatal and adult testes, when compared to other mouse tissues. Within the subsets of spermatogenesis cell types, *N-Ras* is most highly expressed in type A spermatogonia, (enriched in spermatogonial stem cell culture [SSC]), decreasing in type B spermatogonia and slowly rising throughout the continuation of spermatogenesis.

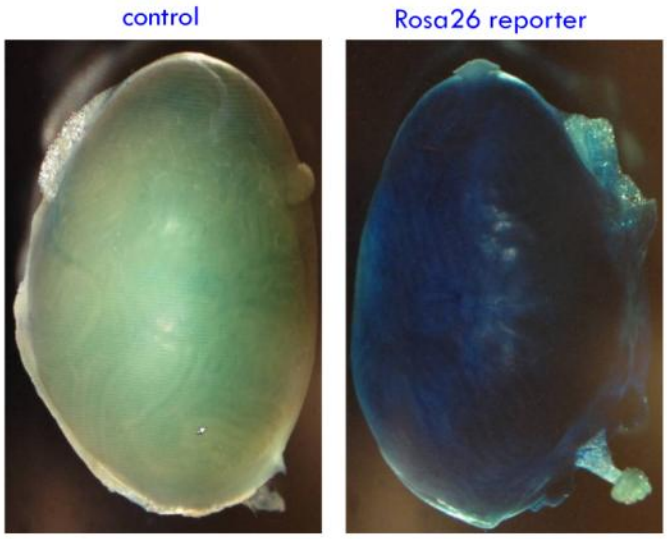

Figure 5.2) Beta-galactosidase expression in *Vasa-CreERT2*; *Rosa26* reporter mice after TAM induced Cre recombination. The validation of Vasa-CreERT2 mediated recombination was observed through the use of *Rosa26* reporter mice. Light (nonspecific) background staining was observed in the interstitial Leydig cells of both TAM negative and Cre negative control testes.

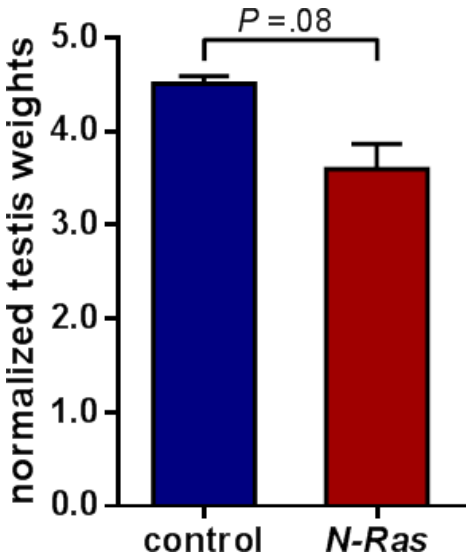

Figure 5.3) *N-Ras Q61R* testis weights appear to be small relative to sibling controls (n=3). Testis weights were normalized to total body weight. Although statistical significance at a 0.05 confidence interval was not achieved by unpaired T-test, the smaller observed size is consistent with the observed phenotype of abnormal spermatogenesis.

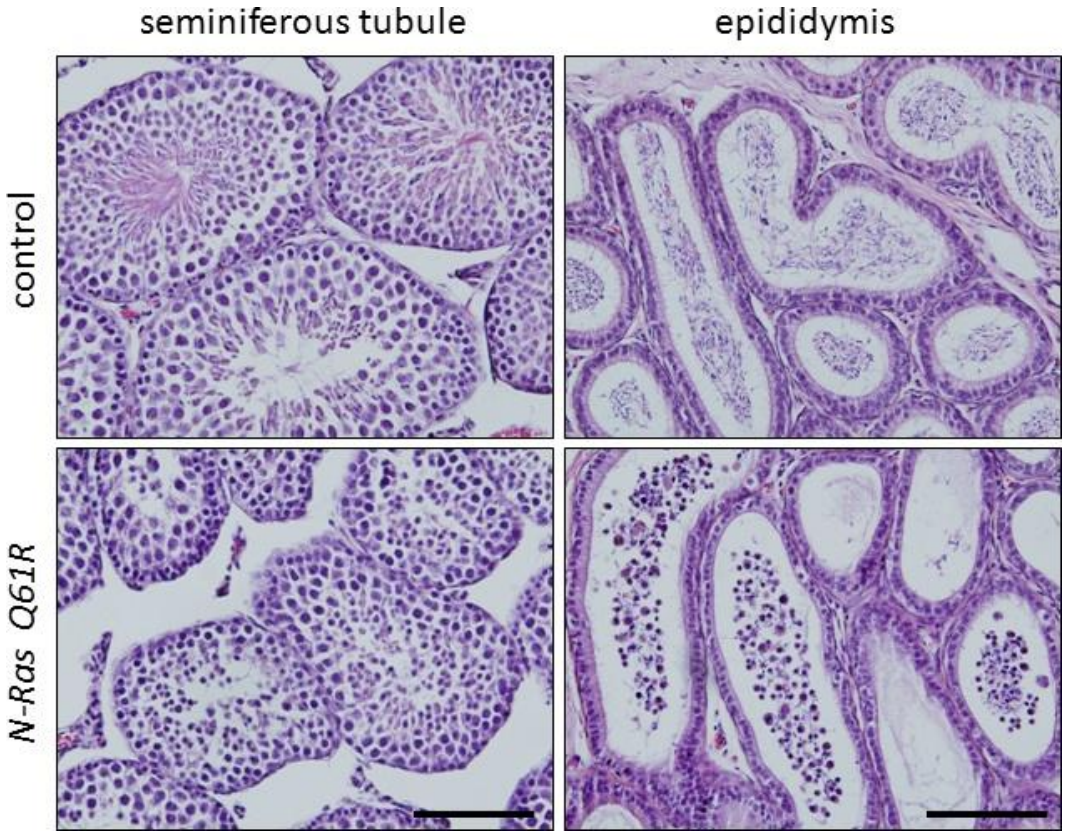

Figure 5.4) Histological analysis of *N-Ras Q61R* mice reveal severe defect in spermiogenesis. H&E stained tissue sections from testes and epididymides of three month-old *N-Ras Q61R* and sibling control mice. Seminiferous tubules of experimental mice lacked elongated spermatids. The block in elongation was also observable as an abnormal accumulation of round cells in the epididymis of experimental mice. Bar = 50 microns.

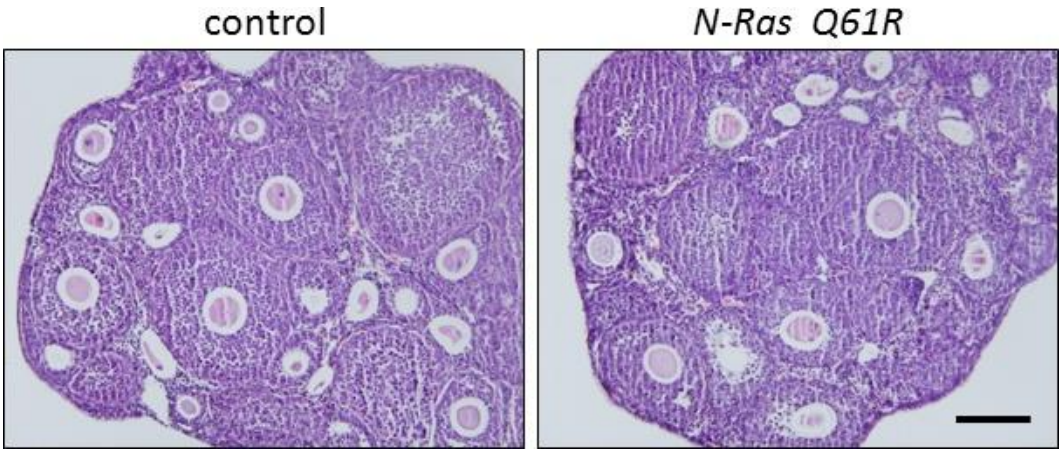

Figure 5.5) Histological analysis of *N-Ras Q61R* mice revealed normal oogenesis. The constitutive activation of *N-Ras* in the oocyte did not have any observable effect on the formation and maturation of follicles. Bar = 250 microns.

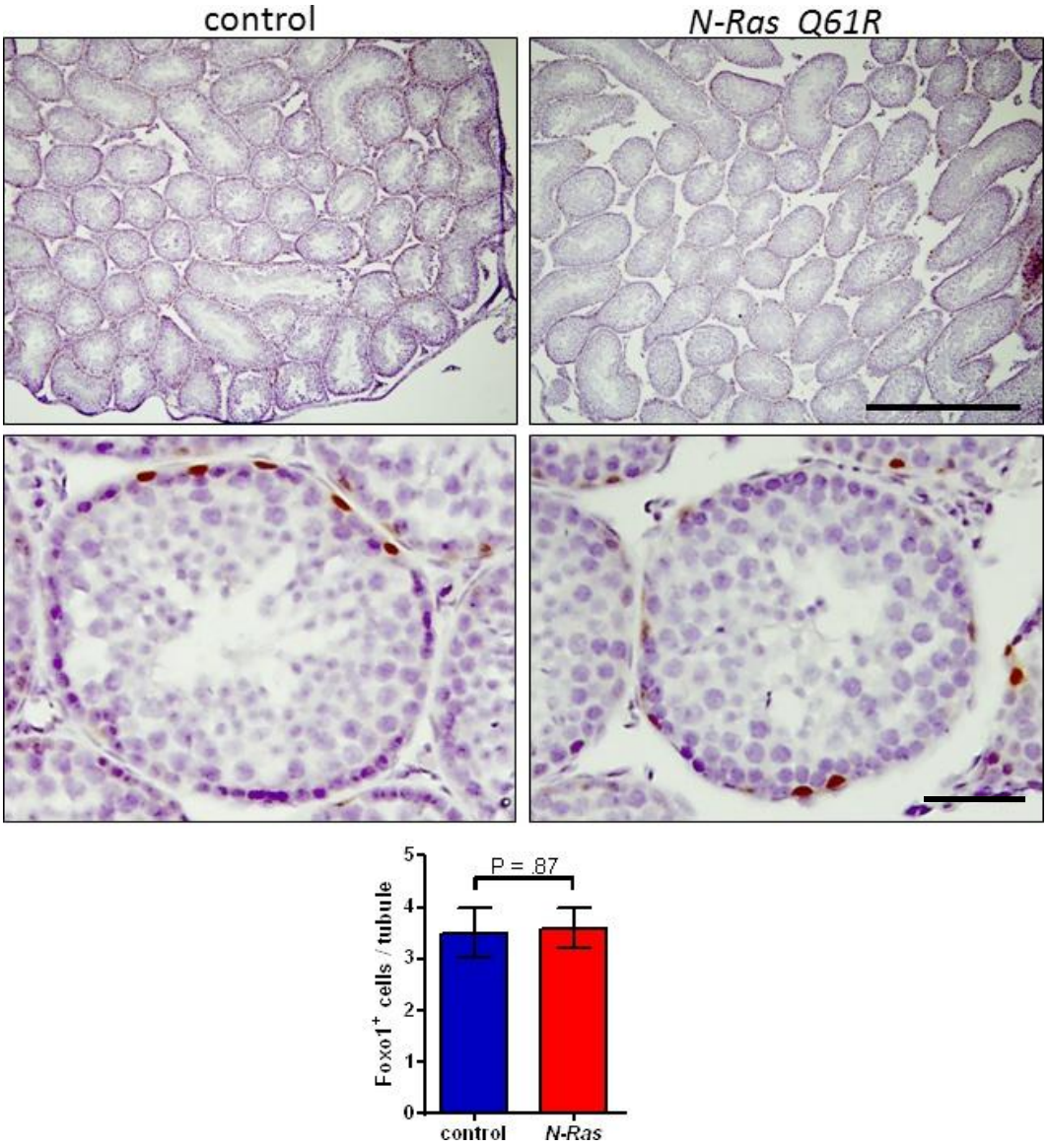

Figure 5.6) Foxo1 immunostaining confirms a normal pool of undifferentiated spermatogonia. Low magnification view of Foxo1 immunostains of three month old *N-Ras Q61R* and control testes (Bar = 500 microns) as well as high magnification view of a single tubule cross section (Bar = 100 microns). Quantification of Foxo1 positive cell counts in twenty tubules revealed no significant change by unpaired T-test.

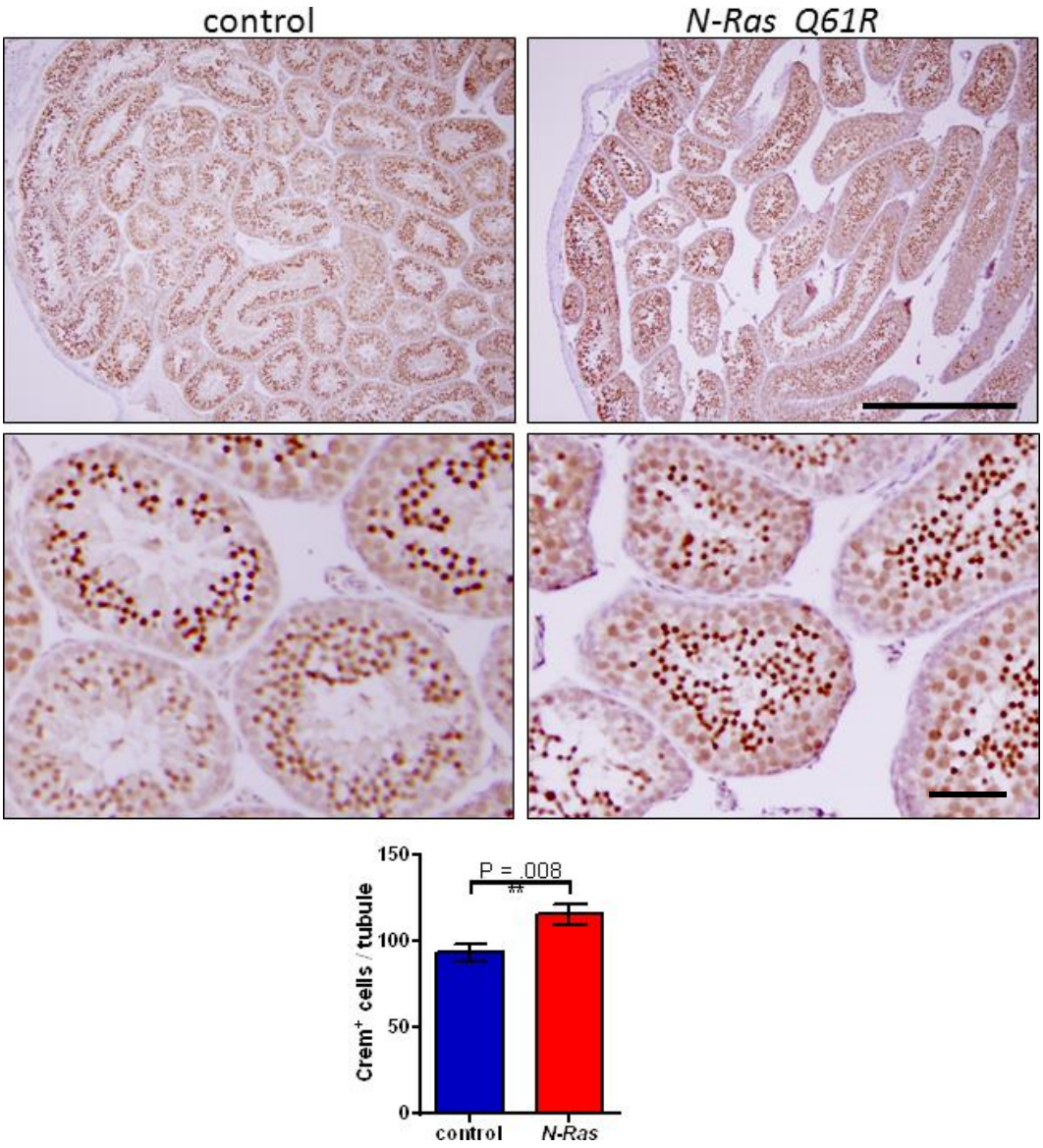

Figure 5.7) Immunostaining for Crem1 reveals a block in spermiogenesis and an accumulation of round spermatids. Both low and high magnification photomicrographs of Crem1 immunostains of three month old *N-Ras Q61R* and control testes. Bar = 500 microns and 100 microns respectively. Quantification of Crem1 positive cell counts in twenty tubules revealed a significant increase by unpaired T-test; $^{**}P < .05$

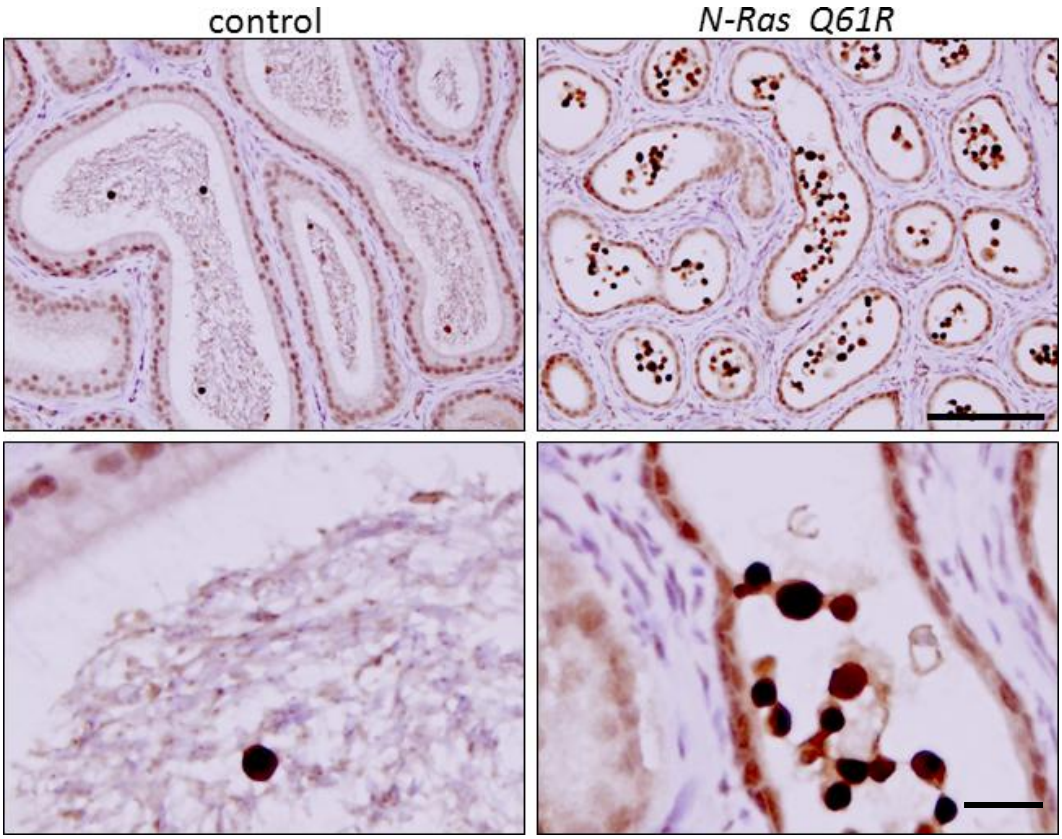

Figure 5.8) Crem1 staining of *N-Ras Q61R* and control epididymis. Both low and high magnification photomicrographs of Crem1 immunostains confirm that the round cells found in the lumen of *N-Ras Q61R* epididymis correspond to spermatids. Bar = 500 microns and 50 microns respectively.

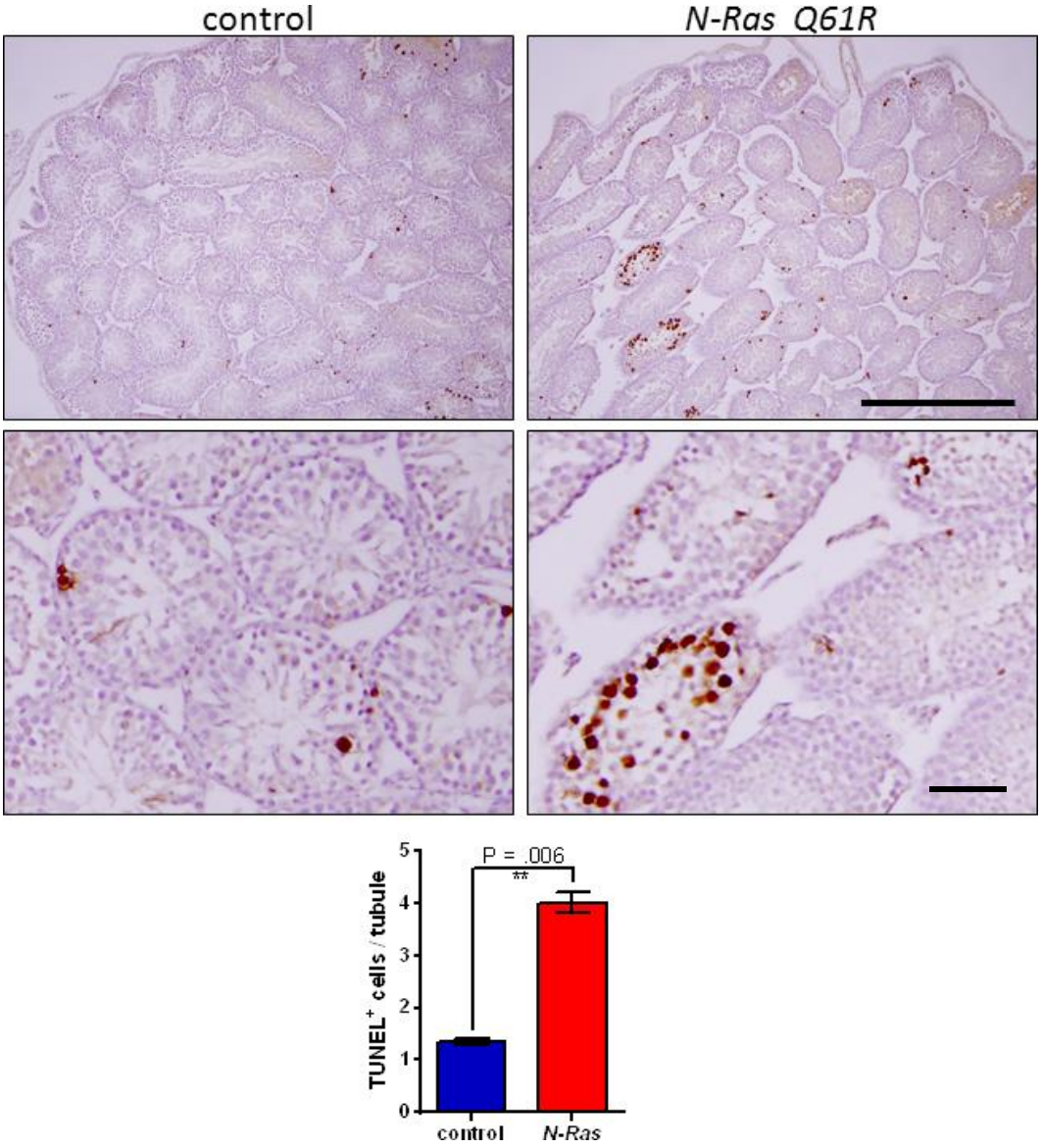

Figure 5.9) TUNEL staining reveals increased apoptosis in seminiferous tubules.

The number of apoptotic cells per tubules increases in *N-Ras Q61R* testes. Low magnification provides a survey of many tubules. Bar = 500 microns. High magnification images details a *N-Ras Q61R* tubule undergoing massive spermatid apoptosis. Bar = 100 microns. Quantification of TUNEL positive cell counts in twenty tubules revealed a significant increase by unpaired T-test; ***P* < .05

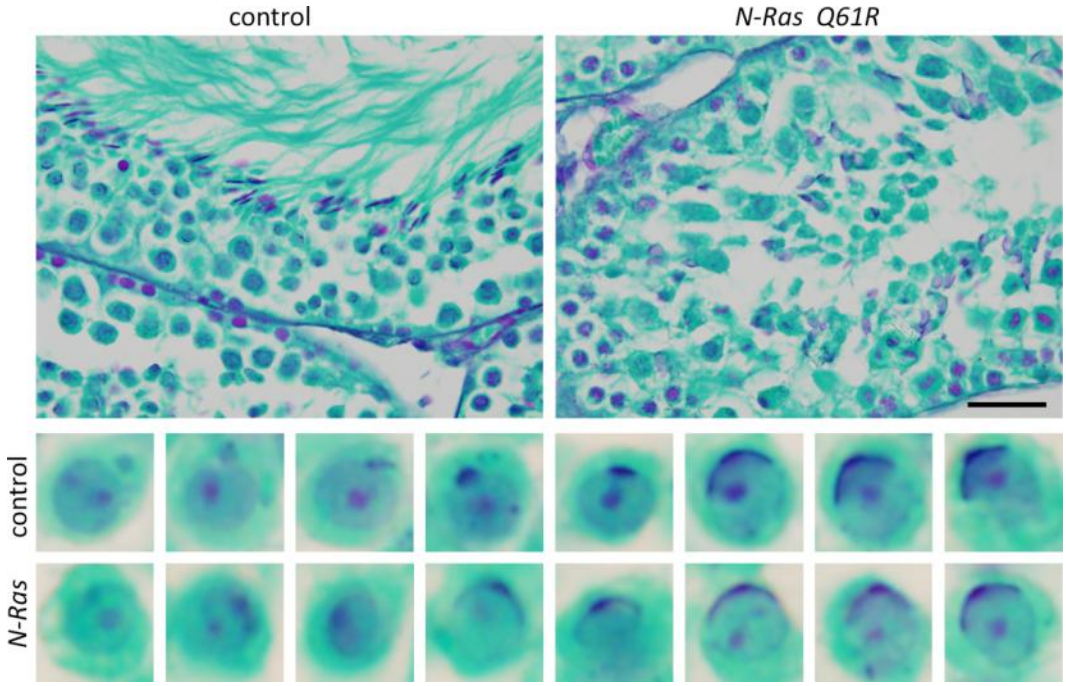

Figure 5.10) PAS-Feulgen staining of seminiferous tubules reveals normal acrosome formation in round spermatids of *N-Ras* Q61R mice. PAS-Feulgen staining of the poly-saccharide rich acrosome (dark purple). Bar = 100 microns. Enlarged spermatids illustrate the migration of the Golgi-derived vesicles to the nuclear membrane and the encapsulation of the anterior end of the nucleus. This process was unaffected in *N-Ras Q61R* spermatids.

CHAPTER SIX

Results

GENE EXPRESSION IN NEONATAL OVARIES PROVIDES REGULATORY CANDIDATES FOR PRIMORDIAL FOLLICLE ACTIVATION

Introduction

The global PFA phenotype was first described a decade ago by Castrillon et al. in a study demonstrating that in *Foxo3* global knockout ovaries, the pool of primary follicles underwent global primordial follicle activation immediately after birth, leading to the accelerated depletion of primordial follicles (Castrillon *et al.* 2003). Prior to these experiments, defects in human ovarian function related to primordial follicles (i.e. premature ovarian failure and primary amenorrhea) were thought to fall into two categories. 1) an increased rate of oocyte apoptosis or 2) a decrease in the initial endowment of primordial follicles (**Fig 6.1**). Currently, *Foxo3* serves as the archetype of a third, now classical, model of premature ovarian failure in mice, sharing the phenotype with a small hand full of genes, including *Pten*, *Tsc1* and *Tsc2* (John *et al.* 2008, Reddy *et al.* 2008, Adhikari *et al.* 2009, Adhikari *et al.* 2010). *Foxo3* has since been conditionally ablated in the embryonic oocyte as well as the adult oocyte, each experiment resulting in global PFA (John *et al.* 2008). Observation of the subcellular localization of Foxo3 revealed a cytoplasmic to nuclear shift during the first three days after birth. The timing of Foxo3 nuclear relocalization coincides with the formation of the primordial follicle, corresponding with the precise moment at which follicle activation must be repressed to preserve the follicle pool (John *et al.* 2008). Conversely, Foxo3 is exported to the cytoplasm and degraded during the primordial to primary follicle transition. The major

regulator of the Foxo transcription factors within the oocyte, PKB (also known as AKT), is responsible for the phosphorylation of Foxo3, which initiates the nuclear export and ultimately ubiquitin mediated degradation (**Fig 6.2**) (Matsuzaki *et al.* 2003, John *et al.* 2008). This apparent nuclear dependency of Foxo3 strongly implicates a role in gene expression regulation as the molecular mechanism underlying PFA repression.

Foxo3 regulated genes have been identified through the use of a constitutively activated Foxo3 mutant fused to the inducible ligand-binding domain of the estrogen receptor (Bakker *et al.* 2007, Eijkelenboom *et al.* 2013). These studies, however, were performed *in vitro* with colon cancer and erythrocyte cell lines, greatly limiting the inferences that can be made regarding the regulation of gene expression in the primordial follicle. With that said, several interesting putative targets do arise from these data including *Kit*, *Igf1-R*, *Irs2*, and *Raptor*, all of which are upregulated by Foxo3 (Bakker *et al.* 2007, Eijkelenboom *et al.* 2013). Each of these candidates plays an important role in the well-established regulation of PI3K and mTOR signaling. However, the missing connection between Tsc1/2 and Pten/Foxo3 is yet to be identified. In addition to the interactions of the PI3K and mTOR signaling pathways, a number of pertinent questions remain ranging from the ligand responsible for pathway activation to the downstream transcriptional targets of Foxo3 (**Fig. 6.3**).

Gene expression profiling: an overview

Gene expression profiling serves as a powerful tool for the unbiased investigation of multiple hypotheses in a single experiment. Specifically, the studies described in this dissertation employed gene expression microarray to detect changes between *Vasa-Cre; Foxo3* ovaries and sibling matched controls. Additionally, arrays were performed to

detect changes in wild-type ovarian gene expression across multiple developmental time points (PD3, PD7, PD14 and PD21). In contrast to quantitative PCR, which limits experiments to a relatively small list of candidate genes, microarray technology allows for the detection of global changes in gene expression, limited only by the current knowledge of gene transcription products. For these studies the Illumina MouseRef-8 BeadChip was chosen to allow for powerful detection of gene expression changes in 24,854 well-established protein coding transcripts. Compared to the MouseWG-6 BeadChip, many of the more provisional transcripts were sacrificed to make room for two additional samples per chip. This provided an increase in statistical power through the inclusion of an additional biological replicate per experimental group.

To obtain the highest quantity and quality of RNA from the limited tissue of a neonatal ovary, the convenience of RNA extraction kits was forgone in exchange for guanidinium thiocyanate-phenol-chloroform extraction, which provided a greater yield and higher purity of total RNA. For PD3, PD7, and PD14 time points, a single pair of ovaries provided a sufficient quantity of RNA for microarray analysis. However, four pairs of PD1 ovaries were pooled per sample due to their extremely small size. The RNA quality was preserved through rapid dissection technique as well as careful prevention of RNase contamination. Prior to microarray processing, the mRNA quality was assessed through spectrophotometer analysis of 260/230 nm maximum absorption ratio to detect sample contamination. Additionally, micro-channel electrophoresis was performed to measure ribosomal RNA peaks to ensure minimal RNA degradation. A RNA integrity number (RIN) score was calculated for each sample and only samples scoring greater than 9.0 were used for microarray analysis. After RNA integrity and purity was verified, the cRNA is prepared for hybridization. The incorporation of biotinylated UTP facilitates the florescent labeling with Cy3-streptavidin. Quantities of ovarian RNA were sufficient

to avoid RNA amplification, which often introduces artifacts due to the non-linear amplification of different products (Kerkhoven *et al.* 2008). Samples were then hybridized to the BeadChip and scanned to collect raw data.

Gene expression microarray data often presents challenges of data analysis and interpretation. The standard strategy follows four main steps before one can mine the results for meaningful conclusions. These steps include 1) normalization 2) quality control 3) differential comparison and 4) statistical significance. Normalization is employed to remove non-biological differences between samples which are often introduced by technical artifacts or human variation. Quantile normalization can be used under the assumption that the majority of genes are not differentially express and that the sample distributions should be the same across all samples (Bolstad *et al.* 2003). While several nonlinear normalization methods are available, variations between methods are small and quantile normalization is relatively quick to perform. The complete probe set for each sample is ranked by intensity and placed into columns. Each value is replaced by the average of the corresponding row. Finally, the probe sets are restored to the original order, however, the means and distributions of each sample are now equal. While this does not change the rank order of probe intensities within a sample, it provides a more accurate comparison of gene expression between replicates and experimental groups.

Quality control is performed by the analysis of both positive and negative control probe sets. Controls are either sample-independent (relying on spike-in oligonucliotides) or sample-dependent (typically ubiquitously expressed housekeeping genes). An inconsistency within sample-independent controls indicates general errors with sample processing, while sample-dependent controls ensure consistent sample quality. Other quality control tests depend on signal-to-noise ratio and number of genes detected. If multiple probes exist for a single transcript, the transcript average is obtained which is in

turn averaged between biological replicates. Signal intensities can then be compared and genes ranked by greatest fold change.

Finally, statistical significance must be established. Taking into account the number of replicates and the variation within the measurement, a *P*-value is calculated determining the probability that the null hypothesis is true. Further action is required to account for the large number of false positives inherent in high-throughput testing due to the large number of comparisons performed with a microarray. This is often accounted for with the Bonferroni correction, due to its simplicity, which divides the null hypothesis rejection threshold by the number of comparisons made in a single test. This can result in a drastic cut in significant events, which has led many to prefer the more lenient Benjamini-Hochburg false discovery rate correction (Benjamini & Hochberg 1995). Performed and analyzed correctly, microarrays can provide a deep reservoir of data that will generate multiple hypotheses for further investigation.

Replication of global PFA phenotype

The global PFA phenotypes of *Foxo3*, *Pten*, and *Tsc1* were individually replicated to confirm reproducibility previous to microarray profiling. Experimental ovaries and sibling matched controls were paraffin embedded at multiple time points (PD7, PD14, and PD21) to serve as a valuable resource for immunohistological validation of microarray results as well as future investigations. The dramatic global PFA phenotype was observed by histological analysis of each time point (**Fig. 6.4**).

Changes in gene expression are minimal in Vasa-Cre; Foxo3 PD3 ovaries.

To identify changes resulting from the loss of *Foxo3* in the oocyte, mRNA expression profiles of *Vasa-Cre*; *Foxo3* PD3 ovaries were compared to littermate controls. RNA was isolated from pairs of PD3 ovaries to detect the primary changes of gene expression that occur in the earliest stages of primordial follicle activation. This comparison provided strikingly few statistically significant changes in gene expression which can be visualized by graphing control vs. experimental expression values (**Fig 6.5**). The five genes which passed statistical tests are listed below (**Table 6.1**) but all differences observed fell below the 1.5 fold change threshold, which is generally considered the lower limit of accurate detection by microarray. While changes in gene expression were hypothesized due to the observed nuclear relocalization of Foxo3, the PD3 time point chosen appears to be premature. Later time points, namely PD4, would certainly provide greater differences in gene expression but expression profiles must be performed before secondary gene expression changes, resulting from oocyte and granulosa cell maturation, obscure the transcriptional network responsible for PFA.

Gene expression profiling of neonatal ovaries provides an extensive list of differentially expressed genes throughout early ovary development.

A second experimental design aimed to identify changes in gene expression during neonatal ovarian development. These arrays were performed as previously described and comparisons were made between each successive time points (PD1 vs. PD3, PD3 vs. PD7, and PD7 vs. PD14). These comparisons resulted in substantial number of differentially expressed genes, several of which play known roles in ovarian function. Multiple genes with known ovarian function, including *Oct4*, *Zp1, Zp3, Oosp1*

and *Omt2b*, serve as yet another level of positive controls validating the effectiveness of microarray analysis. 91 genes were determined to be differentially expressed (>1.5 fold change) between PD1 and PD3 ovaries, of which the top 25 are ranked below (**Table 6.2**). Multiple PFA regulatory candidates can be "cherry-picked" based on potential roles in PI3K and mTOR signaling including *Gdf9* and *eIF4E-1B*. Growth differentiation factor 9 (*Gdf9*), is an oocyte-derived factor previously shown to activate the PI3K pathway in granulosa cells to provide resistance to apoptosis in cultured preantral follicles (Orisaka *et al.* 2006). Global *Gdf9* KO results in a primary follicle arrest phenotype reminiscent of the *Kit* mutations described above (Hayashi *et al.* 1999). The observed *in vivo* expression in primordial follicles may also play a role in the oocyte/granulosa cell signaling and PFA regulation. *eIF4E-1B* is particularly interesting as it is an ovarian expressed homolog of *eIF4E-1*, a downstream member of the mTORC1 mediated translational regulation machinery. Interestingly, mammalian eIF4E-B1 expression is limited the oocyte and may provide oocyte specific regulation of translation (Evsikov *et al.* 2006). In the zebrafish ovary, data suggests that, despite *eIF4E-1* homology, *eIF4E-1B* may serve an alternative function, as it does not appear to function in the same manner as eIF4E-1 which interacts with eIF4G and 4E-BPs to bind the 5' cap of regulated mRNAs (Robalino *et al.* 2004). In addition to providing insights into the biology of PFA, these gene expression profiles of neonatal ovaries may also serve to generate hypotheses regarding follicle formation as well as oocyte and granulosa cell maturation.

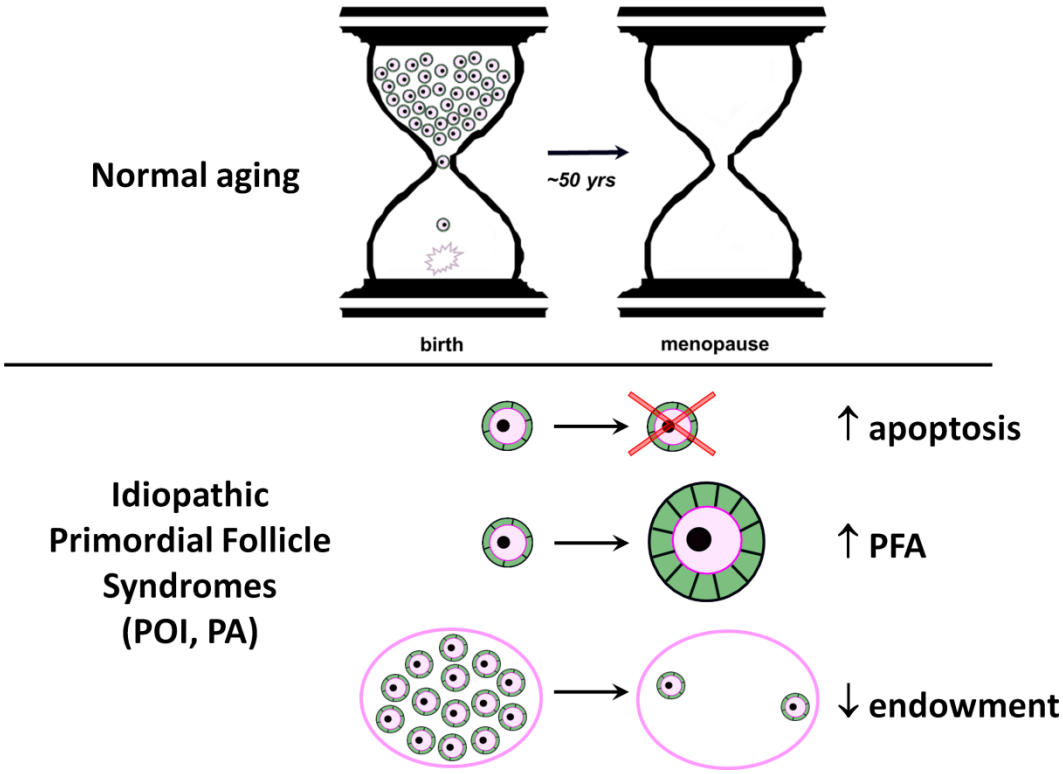

Figure 6.1) Normal ovarian aging compared with three hypothetical mechanisms of premature ovarian failure. The human ovary is born with a finite number of oocytes, which define a woman's reproductive years. Under normal circumstances, that pool of oocytes will last from puberty until about fifty years of age. Three mechanisms underlying premature ovarian insufficiency (a.k.a. premature ovarian failure) and primary amenorrhea are illustrated. 1) an increase rate of oocyte apoptosis, 2) an increased rate in PFA, and 3) an insufficient endowment of initial follicles.

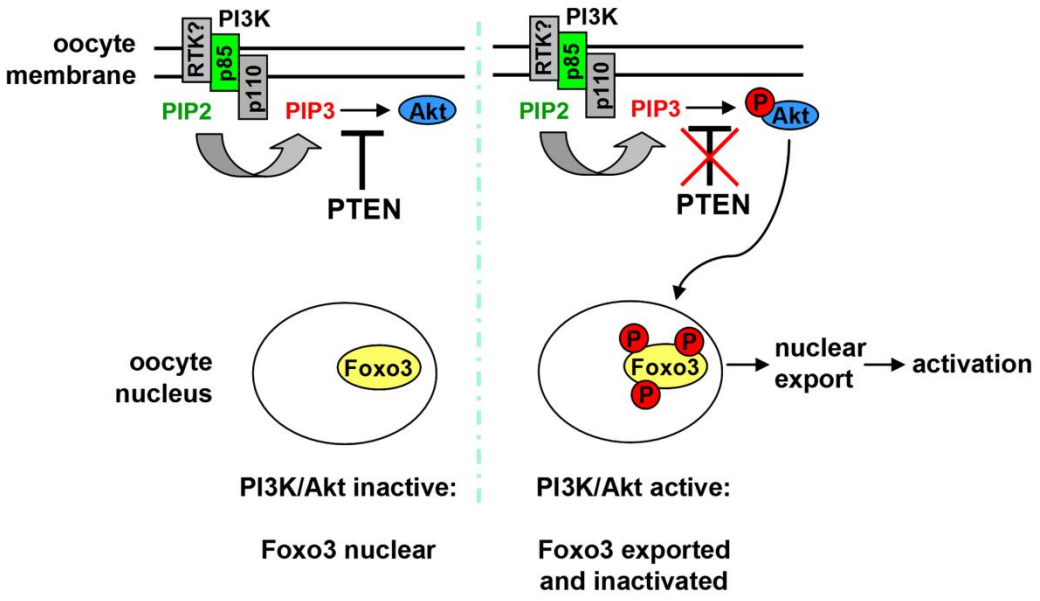

Figure 6.2) PI3K signaling via Foxo3 controls follicle activation and quiescence. Foxo3 serves as a molecular switch controlling primordial follicle activation. Upon activation of PI3K signaling, AKT phosphorylation initiates the nuclear export of Foxo3, consequently turning off the Foxo3 transcriptional regulation and thus inducing PFA.

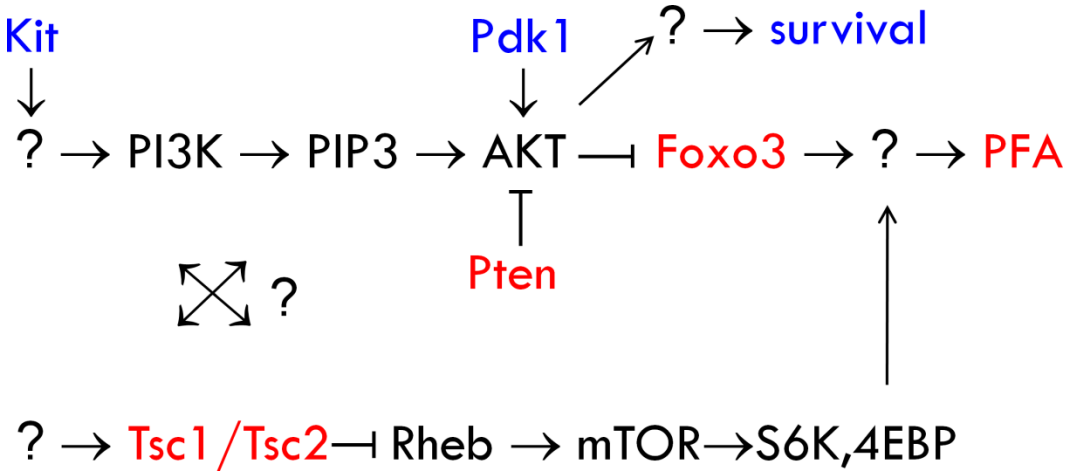

Figure 6.3) Interactions between known regulators of primordial follicle activation. A very limited number of genes have been shown to have a regulatory effect on the survival and activation of the primordial follicle. Genes shown in red have specifically been shown to cause global PFA upon conditional ablation in the oocyte. Mutations in *Kit* and *Pdk1* result in accelerated clearance of the primordial follicle pool; however, this does not occur by increased PFA. Question marks indicate important gaps in the full understanding of PFA regulation, including pathway activators and downstream effectors.

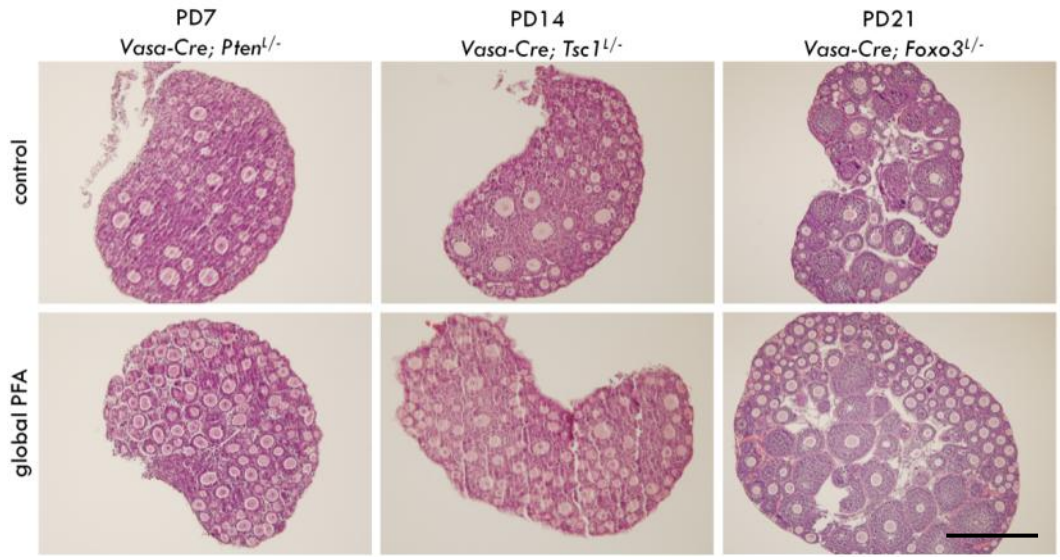

Figure 6.4) Replication of global PFA phenotypes. The global PFA phenotype observed in response to oocyte loss of *Pten*, *Tsc1 or Foxo3* was replicated and ovaries were collected for PD7, PD14, and PD21 time points. By PD7, global PFA is observed in H&E stained sections as all follicles have reached the primary stage. The increased size of the global PFA ovary is noticeable by PD14 and dramatically increases by PD21. Bar = 500 microns.

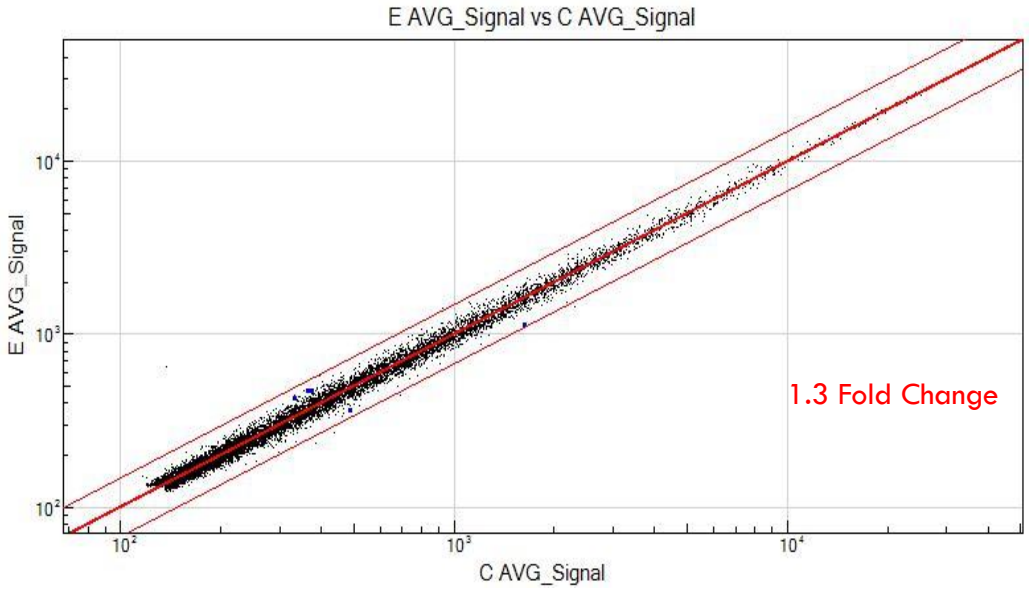

Figure 6.5) Graphical summary of total gene expression data demonstrates the similarity in expression profiles between *Vasa-Cre; Foxo3*$^{L/-}$ and *Vasa-Cre* negative *Foxo3*$^{L/-}$ control ovaries. Each point, representing a single gene probe, has been graphed as the average signal in the control group vs. the average signal in the experimental group. The center red line indicates no change whereas the outer lines designate the 1.3 fold threshold. Five genes, found in Table 6.1, exceeded this threshold.

Table 6.1) Differentially expressed genes between PD3 *Vasa-Cre; Foxo3* ovaries compared to sibling controls.

Symbol	Gene Name	Abs Fold Change (cKO vs wt)	Direction
Col6a	collagen 6A	1.39	Down
Mtf1	metal-regulatory transcription factor 1	1.28	Down
Nudc	nuclear distribution C homolog	1.34	Up
Sec23a	SEC23-related protein A	1.32	Up
Wwp2	WW domain containing E3 ubiquitin protein ligase 2	1.29	Up

Table 6.2) Top 25 differentially expressed genes between PD1 and PD3 ovaries.

Symbol	Gene Name	Abs Fold Change (PD3 vs PD1)	Direction
Zp3	zona pellucida glycoprotein 3 (sperm receptor)	5.53	Up
Oas1d	2'-5' oligoadenylate synthetase 1D	4.08	Up
Zp1	zona pellucida glycoprotein 1 (sperm receptor)	3.56	Up
Nlrp14	NLR family, pyrin domain containing 14	3.24	Up
Dppa5	developmental pluripotency associated 5	2.89	Up
Padi6	peptidyl arginine deiminase, type VI	2.86	Up
Oosp1	oocyte secreted protein 1	2.81	Up
Gdf9	growth differentiation factor 9	2.80	Up
Mfap5	microfibrillar associated protein 5	2.41	Up
Xdh	xanthine dehydrogenase	2.41	Up
Cpb2	carboxypeptidase B2 (plasma)	2.34	Up
Npm2	nucleophosmin/nucleoplasmin 2	2.33	Up
Fetub	fetuin beta	2.32	Up
Actg2	actin, gamma 2, smooth muscle, enteric	2.26	Up
Tsga8	testis specific gene A8	2.23	Down
Bcl2l10	BCL2-like 10	2.21	Up
Omt2b	oocyte maturation, beta	2.14	Up
Ddx25	DEAD (Asp-Glu-Ala-Asp) box helicase 25	2.14	Down
Ap3b2	adaptor-related protein complex 3, beta 2 subunit	2.09	Up
Ogn	osteoglycin	2.06	Up
Oas1c	2'-5' oligoadenylate synthetase 1C	2.06	Up
Map3k6	mitogen-activated protein kinase kinase kinase 6	2.05	Up
Spo11	sporulation protein, meiosis-specific	2.05	Down
Agpt2	Angiopoietin 2	2.04	Down
Rfpl4	ret finger protein-like 4A	2.04	Up

CHAPTER SEVEN

Conclusions and Recommendations

Rheb is indispensable for spermatogenesis but is not required for oogenesis

These studies document a male infertility phenotype associated with multiple defects in the meiotic and post-meiotic stages of spermatogenesis in mice with conditional genetic inactivation of *Rheb* in the germ line. Interestingly, given prior studies implicating mTORC1 in stem cell self-renewal, *Rheb* was dispensable for spermatogonial self-renewal and mitotic proliferation (Hobbs *et al.* 2010). However, *Rheb* was necessary for spermiogenesis, as *Rheb* males exhibited greatly reduced epididymal sperm numbers, and the few sperm present were immotile and exhibited grossly abnormal head morphology. A delay in meiotic progression was also evident at two months of age as spermatocyte counts were significantly increased. Immunostains for meiotic initiation-associated double-strand DNA breaks were relatively unaffected, further suggesting that these defects were due to delays or abnormalities in meiotic progression, and not meiotic initiation per se. Interestingly, these pleiotropic phenotypes were age-dependent, and in five month-old males, the meiotic defect was even more severe, with greatly decreased numbers of post-meiotic spermatids.

A large number of mouse mutants with combined defects in meiosis and spermiogenesis have been described. These mutations affect a wide range of processes, from acrosome and tail formation to misregulation of late spermiogenesis gene expression (Yan 2009). The multiple defects that I have described resemble in several respects the spermatogenesis phenotype previously described for mice with conditional

germ line inactivation of *Dicer*, the miRNA processing enzyme (Korhonen *et al.* 2011, Romero *et al.* 2011). The *Dicer* cKO is also infertile due to cumulative defects in meiosis and spermiogenesis that result in an oligoasthenoteratozoospermia phenotype. Delayed progression of meiosis was also observed but the phenotype was manifest during the first wave of spermatogenesis and did not worsen with age (Romero *et al.* 2011). Both Rheb and Dicer control critical pathways regulating protein expression, albeit through two fundamentally different mechanisms. The biological basis of these *Rheb* and *Dicer* male infertility phenotypes likely resides in this precise regulation of gene expression required to complete the complex transcription-independent processes of meiotic and post-meiotic sperm development. With hundreds of testis-specific genes expressed in spermatocytes and spermatids, the translation of these mRNAs must be perfectly orchestrated to coordinate acrosome biogenesis, tail formation, nuclear condensation and cytoplasm removal. With the loss of functional spermatozoa in *Vasa-Cre; Rheb*$^{f/-}$ in the testis, it is a reasonable to hypothesize that regulation of protein translation by mTORC1 is required for spermiogenesis. Although I did not document an obvious defect in spermatogonial function, and the numbers of these cells were unaffected, it is possible that Rheb inactivation resulted in some unidentified abnormality (metabolic, transcriptional, etc.) in early stages of spermatogenesis that became manifest at later steps of spermatogenesis.

With regards to the control of protein translation, Rheb and mTORC1 act through canonical pathways including the phosphorylation of 4EBP and S6K. I was unable to document, by in situ methods or Western blotting, significant alterations in the phosphorylation state of these key mTOR effectors. Several possibilities may be considered. First, by Western blotting, the significant somatic cell contamination of whole testes lysates could make it difficult to detect differences in phosphorylation levels (I observed no differences through these methods - unpublished data). I also failed to

detect differences in the phosphorylation levels in these factors (and hence significant alterations in mTORC1 signaling) by potentially more sensitive in situ methods, although immunohistochemistry may also be insensitive to relatively modest changes in target epitope levels. It is also possible that unknown feedback loops serve to preserve Tsc/mTOR signaling in the absence of Rheb. Although a precise molecular mechanism of action was not determined, the *Rheb* cKO is the first genetic *in vivo* study which implicates Rheb in the regulation of spermatogenesis.

Despite the complete sterility of *Rheb* cKO males, cKO females were fertile and exhibited normal fecundity. I observed no alterations in primordial follicle numbers, or follicle maturation, by careful histologic analyses. This result is somewhat surprising in light of previous studies clearly demonstrating a central role of mTOR signaling in the regulation of primordial follicle activation. The global follicle activation phenotype previously documented in *Tsc1* or *Tsc2* cKO females was associated with dramatic upregulation of the mTOR signaling pathway (demonstrable with the same immunohistochemical assays performed in our study) (Adhikari *et al.* 2009, Adhikari *et al.* 2010), yet *Rheb* conditional inactivation in oocytes did not have any observable effect on follicle maturation. Although different Cre deletor lines were used in these studies, this does not appear to provide an adequate explanation, as both Cre deletor lines have been extensively utilized and well-documented to lead to efficient Cre-mediated recombination in primordial oocytes (Castrillon *et al.* 2003, Lan *et al.* 2004, Gallardo *et al.* 2007, Adhikari *et al.* 2009). If mTORC1 activation played an essential role in the recruitment of primordial follicles, then Rheb inactivation would be predicted to result in a primordial follicle arrest phenotype in the absence of mTOR signaling secondary to Rheb inactivation. Explanations for the lack of phenotype may include the action, within the oocyte, of functionally-redundant members of the GTPase superfamily, such as the

Rheb homolog RhebL1. Although global *RhebL1* knockout mice were viable and fertile (Zou *et al.* 2011), I have documented *RhebL1* expression in the oocyte, which could serve to compensate for the failure of complete Rheb inactivation to affect any necessary thresholds of mTOR activation (Tee *et al.* 2005). A *Rheb* germ cell cKO in a *RhebL1* null background may provide insights into this hypothesis. Alternately, an unknown Rheb homolog, or perhaps a more distantly-related Ras-like GTPase may provide this function. Furthermore, cellular functions including the control of apoptosis, differentiation, and the actin cytoskeleton regulation have been proposed to be modulated by non-canonical (i.e. mTORC1-independent) functions of Tsc1/Tsc2 (Neuman & Henske 2011) and it is possible that such mTOR-independent actions of the Tsc complex also contribute to the lack of a *Rheb* ovarian phenotype.

Further mechanistic studies should aim to reveal the underlying molecular effect of Rheb cKO

Further investigations of the *Vasa-Cre; Rheb* phenotype should be focused on the identification of both the mechanism of action in spermatogenesis as well as the mechanism of compensation in the ovary. With no change detectable in downstream pathway activation, additional antibodies as well as increased sensitivity will be required before progress can be made from this immunohistological approach. An alternative strategy could attempt the further characterization of the defect in meiotic progression in order to find a separate foothold for the molecular investigation. Observations of early time points may provide valuable insights into the effect of *Rheb* cKO on the initial wave of spermatogenesis. A reduction in developing testis weights at P10, P14, P18 and P24 should be supportive of potential defects in various stages of spermatogenesis such as meiotic entry, meiotic division and round spermatid development. Additionally, flow

cytometry may prove useful for the quantification of the spermatogenesis process based on cellular ploidy (1n, 2n, and 4n) (Hittmair *et al.* 1992). In addition to DNA staining, fluorochromes marking mitochondrial activity and vimentin positivity have be used to differentiate between somatic cells and ten distinct stages of spermatogenesis in testicular suspensions (Suter *et al.* 1997). Quantification of the cellular stages affected in both young and old *Vasa-Cre; Rheb* males will allow for a more detailed description of precise defects in the spermatogenic process.

The age dependent aspect of the *Vasa-Cre; Rheb* phenotype also presents a particularly interesting paradox which could lead to its own line of investigation. Most age-dependent defects in spermatogenesis are disruptions in the delicate balance of SSC self-renewal and differentiation where, over time, the population of SSCs undergoes a gradual decrease or are at some point extinguished, resulting in a germ cell-less phenotype. As the numbers of spermatogonia were unaffected and mitotic entry was observed in all time points, it is clear that the age-dependent defect is not afflicting the stem cell. One possibility could be defective DNA damage repair mechanisms resulting in the accumulation mutations which could trigger meiotic checkpoints. Another potential mechanism could be the loss of telomerase activity which has been demonstrated in response to rapamycin inhibition of mTOR (Zhou *et al.* 2003). TERT, the rate limiting component of telomerase, has been shown to form a complex with PKB, Hsp90, and mTOR which could maintain dependence on Rheb (Kawauchi *et al.* 2005, Sundin & Hentosh 2012).

Conditional activation of N-Ras results in a severe block in spermatid maturation

Vasa-Cre driven expression of the *N-Ras Q61R* constitutively active allele resulted in a severe defect in spermiogenesis. On the other hand, oogenesis appeared to be unaffected as growing follicles of all stages were observed. Gross examination

revealed slightly, yet not significantly, smaller testes. This subtle decrease in testis weight is typical of post meiotic defects in spermatogenesis as the total number of germ cells is not dramatically decreased. Upon histological analysis, a distinct block in spermiogenesis was apparent as round spermatids accumulated, unable to elongate into mature spermatozoa. Mature spermatozoa were also absent from the lumen of the epididymis, replaced by a population of round cell. This population was confirmed as round spermatids as they expressed the round spermatid marker, Crem1. Detailed cell counts, with the aid of expression markers, confirmed the accumulation of round spermatids while the Foxo1 positive undifferentiated spermatogonia were unaffected. An increase in apoptotic cells per tubule was observed by TUNEL staining with several tubules per section undergoing dramatic apoptotic collapse. Additionally, acrosome formation appeared to proceed normally, further narrowing down the defect to the elongation phase of spermiogenesis.

Two notable gene knockouts result in similar arrest of late stage spermiogenesis, *Tbpl1* and *Miwi* (Martianov *et al.* 2001, Deng & Lin 2002). Both phenotypes mimic the loss of spermatid elongation as well as the increase in apoptotic cells per tubule; however neither paper described the presence of round spermatids in the epididymis. *Tbpl1* was determined to control the transcription of multiple spermiogenesis transcripts including *MTEST640, 641,* and *640* (Martianov *et al.* 2001). Miwi was shown to interact with Crem1 to regulate translation required for late spermiogenesis (Deng & Lin 2002). While the phenotypes are similar, a hypothesized connection between any of these three spermatid arrest phenotypes would require more support than can be gleaned from current literature.

In addition to the effect on spermiogenesis, it is important to consider the lack of phenotype in the spermatogonial stem cell as well as in the ovary. While expression in spermatogonia was expected based on gene expression profiles, post-transcriptional

regulation may prevent translation. In the process of composing this discussion a paper was identified which demonstrates a significantly higher expression of N-Ras mRNA in round spermatids compared to pachytene spermatocytes as well as neonatal and adult testis (Sorrentino *et al.* 1988).

Malignant potential of germ cell activation of N-Ras

Due to the oncogenic nature of *N-Ras*, the potential for a malignant phenotype was also present at the onset of these experiments. Activating *N-Ras* mutations are particularly common in skin cancer, as they are found to be the driving force behind 10-20% of melanoma cases (Sosman & Puzanov 2006). *N-Ras* has also been implicated, along with *Kit* and *K-Ras*, in the development of testicular germ cell tumors (TGCT) (Goddard *et al.* 2007). However, due to the post-meiotic nature of this defect there does not appear to be any type of premalignant phenotype but more so a clean arrest in the maturation of non-dividing germ cells. There was no evidence of hyperplasia observed in any *Vasa-Cre; N-Ras Q61R* mouse.

Future directions for the identification of N-Ras function in spermiogenesis

To confirm the expression of the constitutively active N-Ras allele, it may be helpful to document hyperactivity of the Ras/Raf/MEK/ERK pathway; i.e. through detection of increased phospho-ERK. This should be feasible, as antibodies are commercially-available. This may present some of the same challenges faced in the characterization of the *Vasa-Cre; Rheb* phenotype but should be attempted none the less. Transmission electron microscopy has previously been used to describe spermiogenesis defects as it allows for visualization of the complex sub-cellular rearrangements occurring throughout spermiogenesis including manchette microtubules, perinuclear ring

and nuclear condensation (Schnabel *et al.* 2005). Reorganization of the cytoskeleton can also be observed through the staining of F-actin filaments with phalloidin.

Microarray conclusions and future directions

The gene expression profiles described in this dissertation will provide the foundation for multiple lines of inquiry into the regulatory mechanisms behind primordial follicle activation, early follicle growth, and granulosa cell function. Moving forward, additional data analysis can be employed to further capitalize on the significant gene lists obtained. Gene ontology analysis is a useful tool for organizing a long list of differentially expressed genes into groups determined by previously annotated gene functions. This can highlight multiple genes with common roles in biological processes, molecular functions or cellular components, providing a mechanistic overview in addition to narrowing down gene candidates (Ashburner *et al.* 2000).

While little can be done regarding the limited number of differentially expressed genes discovered in the *Vasa-Cre; Foxo3* array, the strategy remains valid. However, a latter time point, perhaps PD4, should be considered to perhaps permit the loss of Foxo3 to more greatly affect mRNA expression and mRNA levels. Alternatively, PD3 may serve as an acceptable time point for other experimental approaches such as ChIP-Seq which would detect changes in Foxo3 binding earlier than changes in gene expression and would obviate potential problems related to indirect changes in gene expression. Comparison to *Vasa-Cre; Tsc1* and *Vasa-Cre; Pten* PD4 testes could unite the two pathways through the identification of shared genes regulated by both mTOR and PI3K signaling.

Conclusion

The investigations described in this dissertation have identified both *Rheb* and *N-Ras* as indispensable for meiotic progression and spermiogenesis, respectively. Additionally, neither *Rheb* nor *N-Ras* were found to play a necessary role in female fertility despite the known role of PI3K and mTOR signaling pathways in the regulation of primordial follicle activation. Prior to these studies, no *in vivo* evidence had been presented demonstrating a spermatogenesis dependency on either of these two pathways. An unbiased approach was also taken to further identify key players in PFA regulation through the gene expression profiling of neonatal wild-type ovaries as well as ovaries in the earliest stages of the classical global PFA phenotype. These findings and future investigations into the underlying mechanisms should lead to important insights into the network of signaling pathways which regulate both spermatogenesis and oogenesis.

BIBLIOGRAPHY

Abou-Haila A & Tulsiani DR 2000 Mammalian sperm acrosome: formation, contents, and function. *Arch Biochem Biophys* **379** 173-182.

Adams GP & Ratto MH 2013 Ovulation-inducing factor in seminal plasma: a review. *Anim Reprod Sci* **136** 148-156.

Adhikari D, Flohr G, Gorre N, Shen Y, Yang H, Lundin E, Lan Z, Gambello MJ & Liu K 2009 Disruption of Tsc2 in oocytes leads to overactivation of the entire pool of primordial follicles. *Mol Hum Reprod* **15** 765-770.

Adhikari D & Liu K 2009 Molecular mechanisms underlying the activation of mammalian primordial follicles. *Endocr Rev* **30** 438-464.

Adhikari D, Zheng W, Shen Y, Gorre N, Hamalainen T, Cooney AJ, Huhtaniemi I, Lan ZJ & Liu K 2010 Tsc/mTORC1 signaling in oocytes governs the quiescence and activation of primordial follicles. *Hum Mol Genet* **19** 397-410.

Akbay EA, Pena CG, Ruder D, Michel JA, Nakada Y, Pathak S, Multani AS, Chang S & Castrillon DH 2013 Cooperation between p53 and the telomere-protecting shelterin component Pot1a in endometrial carcinogenesis. *Oncogene* **32** 2211-2219.

Alberts B, Johnson A & Lewis J 2002 *Molecular Biology of the Cell*. New York: Garland Science

Ashburner M, Ball CA, Blake JA, Botstein D, Butler H, Cherry JM, Davis AP, Dolinski K, Dwight SS, Eppig JT, Harris MA, Hill DP, Issel-Tarver L, Kasarskis A, Lewis S, Matese JC, Richardson JE, Ringwald M, Rubin GM & Sherlock G 2000 Gene ontology: tool for the unification of biology. The Gene Ontology Consortium. *Nat Genet* **25** 25-29.

Bahat A & Eisenbach M 2006 Sperm thermotaxis. *Mol Cell Endocrinol* **252** 115-119.

Bakker WJ, van Dijk TB, Parren-van Amelsvoort M, Kolbus A, Yamamoto K, Steinlein P, Verhaak RG, Mak TW, Beug H, Lowenberg B & von Lindern M 2007 Differential regulation of Foxo3a target genes in erythropoiesis. *Mol Cell Biol* **27** 3839-3854.

Balhorn R 2007 The protamine family of sperm nuclear proteins. *Genome Biol* **8** 227.

Bedell MA, Brannan CI, Evans EP, Copeland NG, Jenkins NA & Donovan PJ 1995 DNA rearrangements located over 100 kb 5' of the Steel (Sl)-coding region in Steel-panda and Steel-contrasted mice deregulate Sl expression and cause female sterility by disrupting ovarian follicle development. *Genes Dev* **9** 455-470.

Benjamini Y & Hochberg Y 1995 Controlling the False Discovery Rate: A Practical and Powerful Approach to Multiple Testing. *Journal of the Royal Statistical Society. Series B (Methodological)* **57** 289-300.

Birchmeier C, Broek D & Wigler M 1985 ras proteins can induce meiosis in Xenopus oocytes. *Cell* **43** 615-621.

Bjork A, Dallai R & Pitnick S 2007 Adaptive modulation of sperm production rate in Drosophila bifurca, a species with giant sperm. *Biol Lett* **3** 517-519.

Bolstad BM, Irizarry RA, Astrand M & Speed TP 2003 A comparison of normalization methods for high density oligonucleotide array data based on variance and bias. *Bioinformatics* **19** 185-193.

Carriere A, Romeo Y, Acosta-Jaquez HA, Moreau J, Bonneil E, Thibault P, Fingar DC & Roux PP 2011 ERK1/2 phosphorylate Raptor to promote Ras-dependent activation of mTOR complex 1 (mTORC1). *J Biol Chem* **286** 567-577.

Caskurlu T, Tasci AI, Samasti M, Bayraktar Z, Cek M & Sevin G 1999 Immature germ cells in semen and their correlations with other semen parameters. *Int Urol Nephrol* **31** 389-393.

Castellano E & Santos E 2011 Functional specificity of ras isoforms: so similar but so different. *Genes Cancer* **2** 216-231.

Castrillon DH, Miao L, Kollipara R, Horner JW & DePinho RA 2003 Suppression of ovarian follicle activation in mice by the transcription factor Foxo3a. *Science* **301** 215-218.

Chang F, Steelman LS, Lee JT, Shelton JG, Navolanic PM, Blalock WL, Franklin RA & McCubrey JA 2003 Signal transduction mediated by the Ras/Raf/MEK/ERK pathway from cytokine receptors to transcription factors: potential targeting for therapeutic intervention. *Leukemia* **17** 1263-1293.

Childs AJ, Cowan G, Kinnell HL, Anderson RA & Saunders PT 2011 Retinoic Acid signalling and the control of meiotic entry in the human fetal gonad. *PLoS One* **6** e20249.

Clerk A, Aggeli IK, Stathopoulou K & Sugden PH 2006 Peptide growth factors signal differentially through protein kinase C to extracellular signal-regulated kinases in neonatal cardiomyocytes. *Cell Signal* **18** 225-235.

de Visser JA & Elena SF 2007 The evolution of sex: empirical insights into the roles of epistasis and drift. *Nat Rev Genet* **8** 139-149.

Dean J 1992 Biology of mammalian fertilization: role of the zona pellucida. *J Clin Invest* **89** 1055-1059.

Delmas V, van der Hoorn F, Mellstrom B, Jegou B & Sassone-Corsi P 1993 Induction of CREM activator proteins in spermatids: down-stream targets and implications for haploid germ cell differentiation. *Mol Endocrinol* **7** 1502-1514.

Deng W & Lin H 2002 miwi, a murine homolog of piwi, encodes a cytoplasmic protein essential for spermatogenesis. *Dev Cell* **2** 819-830.

Dhillon AS, Hagan S, Rath O & Kolch W 2007 MAP kinase signalling pathways in cancer. *Oncogene* **26** 3279-3290.

Dhillon AS, Pollock C, Steen H, Shaw PE, Mischak H & Kolch W 2002 Cyclic AMP-dependent kinase regulates Raf-1 kinase mainly by phosphorylation of serine 259. *Mol Cell Biol* **22** 3237-3246.

Dougherty MK, Muller J, Ritt DA, Zhou M, Zhou XZ, Copeland TD, Conrads TP, Veenstra TD, Lu KP & Morrison DK 2005 Regulation of Raf-1 by direct feedback phosphorylation. *Mol Cell* **17** 215-224.

Eijkelenboom A, Mokry M, de Wit E, Smits LM, Polderman PE, van Triest MH, van Boxtel R, Schulze A, de Laat W, Cuppen E & Burgering BM 2013 Genome-wide analysis of FOXO3 mediated transcription regulation through RNA polymerase II profiling. *Mol Syst Biol* **9** 638.

Eisenbach M & Giojalas LC 2006 Sperm guidance in mammals - an unpaved road to the egg. *Nat Rev Mol Cell Biol* **7** 276-285.

Evsikov AV, Graber JH, Brockman JM, Hampl A, Holbrook AE, Singh P, Eppig JJ, Solter D & Knowles BB 2006 Cracking the egg: molecular dynamics and evolutionary aspects of the transition from the fully grown oocyte to embryo. *Genes Dev* **20** 2713-2727.

Fawcett DW 1975 The mammalian spermatozoon. *Dev Biol* **44** 394-436.

Fingar DC & Blenis J 2004 Target of rapamycin (TOR): an integrator of nutrient and growth factor signals and coordinator of cell growth and cell cycle progression. *Oncogene* **23** 3151-3171.

Fraire-Zamora JJ & Cardullo RA 2010 The physiological acquisition of amoeboid motility in nematode sperm: is the tail the only thing the sperm lost? *Mol Reprod Dev* **77** 739-750.

Fraune J, Schramm S, Alsheimer M & Benavente R 2012 The mammalian synaptonemal complex: protein components, assembly and role in meiotic recombination. *Exp Cell Res* **318** 1340-1346.

Fritsche-Guenther R, Witzel F, Sieber A, Herr R, Schmidt N, Braun S, Brummer T, Sers C & Bluthgen N 2011 Strong negative feedback from Erk to Raf confers robustness to MAPK signalling. *Mol Syst Biol* **7** 489.

Gallardo T, Shirley L, John GB & Castrillon DH 2007 Generation of a germ cell-specific mouse transgenic Cre line, Vasa-Cre. *Genesis* **45** 413-417.

Gallardo TD, John GB, Bradshaw K, Welt C, Reijo-Pera R, Vogt PH, Touraine P, Bione S, Toniolo D, Nelson LM, Zinn AR & Castrillon DH 2008 Sequence variation at the human FOXO3 locus: a study of premature ovarian failure and primary amenorrhea. *Hum Reprod* **23** 216-221.

Goddard NC, McIntyre A, Summersgill B, Gilbert D, Kitazawa S & Shipley J 2007 KIT and RAS signalling pathways in testicular germ cell tumours: new data and a review of the literature. *Int J Androl* **30** 337-348; discussion 349.

Goertz MJ, Wu Z, Gallardo TD, Hamra FK & Castrillon DH 2011 Foxo1 is required in mouse spermatogonial stem cells for their maintenance and the initiation of spermatogenesis. *J Clin Invest* **121** 3456-3466.

Hamer G, Roepers-Gajadien H, Duyn-Goedhart A, Gademan I, Kal H, Buul P & Rooij D 2002 DNA Double-Strand Breaks and -H2AX Signaling in the Testis. *Biol Reprod* **68** 628-634.

Hamilton WD 2001 *Narrow Roads of Gene Land: Evolution of Sex*. New York: Oxford University Press.

Hamilton WD, Axelrod R & Tanese R 1990 Sexual reproduction as an adaptation to resist parasites (a review). *Proc Natl Acad Sci U S A* **87** 3566-3573.

Hayashi M, McGee EA, Min G, Klein C, Rose UM, van Duin M & Hsueh AJ 1999 Recombinant growth differentiation factor-9 (GDF-9) enhances growth and differentiation of cultured early ovarian follicles. *Endocrinology* **140** 1236-1244.

He Z, Jiang J, Kokkinaki M, Golestaneh N, Hofmann MC & Dym M 2008 Gdnf upregulates c-Fos transcription via the Ras/Erk1/2 pathway to promote mouse spermatogonial stem cell proliferation. *Stem Cells* **26** 266-278.

Hirohashi N & Lennarz WJ 2001 Role of a vitelline layer-associated 350 kDa glycoprotein in controlling species-specific gamete interaction in the sea urchin. *Dev Growth Differ* **43** 247-255.

Hittmair A, Rogatsch H, Offner F, Feichtinger H, Ofner D & Mikuz G 1992 Deoxyribonucleic acid flow cytometry and semiquantitative histology of spermatogenesis: a comparative study. *Fertil Steril* **58** 1040-1045.

Hobbs RM, Seandel M, Falciatori I, Rafii S & Pandolfi PP 2010 Plzf regulates germline progenitor self-renewal by opposing mTORC1. *Cell* **142** 468-479.

Holt WV 2011 Mechanisms of sperm storage in the female reproductive tract: an interspecies comparison. *Reprod Domest Anim* **46 Suppl 2** 68-74.

Hosaka T, Biggs WH, 3rd, Tieu D, Boyer AD, Varki NM, Cavenee WK & Arden KC 2004 Disruption of forkhead transcription factor (FOXO) family members in mice reveals their functional diversification. *Proc Natl Acad Sci U S A* **101** 2975-2980.

Inaba K 2011 Sperm flagella: comparative and phylogenetic perspectives of protein components. *Mol Hum Reprod* **17** 524-538.

Jan SZ, Hamer G, Repping S, de Rooij DG, van Pelt AM & Vormer TL 2012 Molecular control of rodent spermatogenesis. *Biochim Biophys Acta* **1822** 1838-1850.

John GB, Gallardo TD, Shirley LJ & Castrillon DH 2008 Foxo3 is a PI3K-dependent molecular switch controlling the initiation of oocyte growth. *Dev Biol* **321** 197-204.

John GB, Shidler MJ, Besmer P & Castrillon DH 2009 Kit signaling via PI3K promotes ovarian follicle maturation but is dispensable for primordial follicle activation. *Dev Biol* **331** 292-299.

John GB, Shirley LJ, Gallardo TD & Castrillon DH 2007 Specificity of the requirement for Foxo3 in primordial follicle activation. *Reproduction* **133** 855-863.

Kawauchi K, Ihjima K & Yamada O 2005 IL-2 increases human telomerase reverse transcriptase activity transcriptionally and posttranslationally through phosphatidylinositol 3'-kinase/Akt, heat shock protein 90, and mammalian target of rapamycin in transformed NK cells. *J Immunol* **174** 5261-5269.

Kerkhoven RM, Sie D, Nieuwland M, Heimerikx M, De Ronde J, Brugman W & Velds A 2008 The T7-primer is a source of experimental bias and introduces variability between microarray platforms. *PLoS One* **3** e1980.

Kerr JB & de Kretser DM 1974 Proceedings: The role of the Sertoli cell in phagocytosis of the residual bodies of spermatids. *J Reprod Fertil* **36** 439-440.

Kierszenbaum AL 2002 Sperm axoneme: a tale of tubulin posttranslation diversity. *Mol Reprod Dev* **62** 1-3.

Kodaki T, Woscholski R, Hallberg B, Rodriguez-Viciana P, Downward J & Parker PJ 1994 The activation of phosphatidylinositol 3-kinase by Ras. *Curr Biol* **4** 798-806.

Kolch W 2000 Meaningful relationships: the regulation of the Ras/Raf/MEK/ERK pathway by protein interactions. *Biochem J* **351 Pt 2** 289-305.

Kondrashov AS 1988 Deleterious mutations and the evolution of sexual reproduction. *Nature* **336** 435-440.

Korhonen HM, Meikar O, Yadav RP, Papaioannou MD, Romero Y, Da Ros M, Herrera PL, Toppari J, Nef S & Kotaja N 2011 Dicer is required for haploid male germ cell differentiation in mice. *PLoS One* **6** e24821.

Lan ZJ, Xu X & Cooney AJ 2004 Differential oocyte-specific expression of Cre recombinase activity in GDF-9-iCre, Zp3cre, and Msx2Cre transgenic mice. *Biol Reprod* **71** 1469-1474.

Laplante M & Sabatini DM 2009 mTOR signaling at a glance. *J Cell Sci* **122** 3589-3594.

Leon J, Guerrero I & Pellicer A 1987 Differential expression of the ras gene family in mice. *Mol Cell Biol* **7** 1535-1540.

Liang CG, Su YQ, Fan HY, Schatten H & Sun QY 2007 Mechanisms regulating oocyte meiotic resumption: roles of mitogen-activated protein kinase. *Mol Endocrinol* **21** 2037-2055.

Longhese MP, Bonetti D, Guerini I, Manfrini N & Clerici M 2009 DNA double-strand breaks in meiosis: checking their formation, processing and repair. *DNA Repair (Amst)* **8** 1127-1138.

Maatouk DM & Capel B 2008 Sexual development of the soma in the mouse. *Curr Top Dev Biol* **83** 151-183.

Martianov I, Fimia GM, Dierich A, Parvinen M, Sassone-Corsi P & Davidson I 2001 Late arrest of spermiogenesis and germ cell apoptosis in mice lacking the TBP-like TLF/TRF2 gene. *Mol Cell* **7** 509-515.

Matsuzaki H, Daitoku H, Hatta M, Tanaka K & Fukamizu A 2003 Insulin-induced phosphorylation of FKHR (Foxo1) targets to proteasomal degradation. *Proc Natl Acad Sci U S A* **100** 11285-11290.

McKay MM & Morrison DK 2007 Integrating signals from RTKs to ERK/MAPK. *Oncogene* **26** 3113-3121.

McLaughlin EA & McIver SC 2009 Awakening the oocyte: controlling primordial follicle development. *Reproduction* **137** 1-11.

Mendoza MC, Er EE & Blenis J 2011 The Ras-ERK and PI3K-mTOR pathways: cross-talk and compensation. *Trends Biochem Sci* **36** 320-328.

Neuman NA & Henske EP 2011 Non-canonical functions of the tuberous sclerosis complex-Rheb signalling axis. *EMBO Mol Med* **3** 189-200.

O'Donnell L, Nicholls PK, O'Bryan MK, McLachlan RI & Stanton PG 2011 Spermiation: The process of sperm release. *Spermatogenesis* **1** 14-35.

Olie RA, Looijenga LH, Boerrigter L, Top B, Rodenhuis S, Langeveld A, Mulder MP & Oosterhuis JW 1995 N- and KRAS mutations in primary testicular germ cell tumors: incidence and possible biological implications. *Genes Chromosomes Cancer* **12** 110-116.

Orisaka M, Orisaka S, Jiang JY, Craig J, Wang Y, Kotsuji F & Tsang BK 2006 Growth differentiation factor 9 is antiapoptotic during follicular development from preantral to early antral stage. *Mol Endocrinol* **20** 2456-2468.

Oulad-Abdelghani M, Bouillet P, Decimo D, Gansmuller A, Heyberger S, Dolle P, Bronner S, Lutz Y & Chambon P 1996 Characterization of a premeiotic germ cell-specific cytoplasmic protein encoded by Stra8, a novel retinoic acid-responsive gene. *J Cell Biol* **135** 469-477.

Parker GA 1982 Why are there so many tiny sperm? Sperm competition and the maintenance of two sexes. *Journal of Theoretical Biology* **96** 281-294.

Parker GA & Pizzari T 2010 Sperm competition and ejaculate economics. *Biol Rev Camb Philos Soc* **85** 897-934.

Parrott JA & Skinner MK 1999 Kit-ligand/stem cell factor induces primordial follicle development and initiates folliculogenesis. *Endocrinology* **140** 4262-4271.

Randerson JP & Hurst LD 2001 A comparative test of a theory for the evolution of anisogamy. *Proc Biol Sci* **268** 879-884.

Reddy P, Liu L, Adhikari D, Jagarlamudi K, Rajareddy S, Shen Y, Du C, Tang W, Hamalainen T, Peng SL, Lan ZJ, Cooney AJ, Huhtaniemi I & Liu K 2008 Oocyte-specific deletion of Pten causes premature activation of the primordial follicle pool. *Science* **319** 611-613.

Robalino J, Joshi B, Fahrenkrug SC & Jagus R 2004 Two zebrafish eIF4E family members are differentially expressed and functionally divergent. *J Biol Chem* **279** 10532-10541.

Romero Y, Meikar O, Papaioannou MD, Conne B, Grey C, Weier M, Pralong F, De Massy B, Kaessmann H, Vassalli JD, Kotaja N & Nef S 2011 Dicer1 depletion in male germ cells leads to infertility due to cumulative meiotic and spermiogenic defects. *PLoS One* **6** e25241.

Schnabel D, Ramirez L, Gertsenstein M, Nagy A & Lomeli H 2005 Ectopic expression of KitD814Y in spermatids of transgenic mice, interferes with sperm morphogenesis. *Dev Dyn* **233** 29-40.

Schneider CA, Rasband WS & Eliceiri KW 2012 NIH Image to ImageJ: 25 years of image analysis. *Nat Methods* **9** 671-675.

Sekido R 2010 SRY: A transcriptional activator of mammalian testis determination. *Int J Biochem Cell Biol* **42** 417-420.

Sherman BM & Korenman SG 1975 Hormonal characteristics of the human menstrual cycle throughout reproductive life. *J Clin Invest* **55** 699-706.

Sorrentino V, McKinney MD, Giorgi M, Geremia R & Fleissner E 1988 Expression of cellular protooncogenes in the mouse male germ line: a distinctive 2.4-kilobase pim-1 transcript is expressed in haploid postmeiotic cells. *Proc Natl Acad Sci U S A* **85** 2191-2195.

Sosman JA & Puzanov I 2006 Molecular targets in melanoma from angiogenesis to apoptosis. *Clin Cancer Res* **12** 2376s-2383s.

Sullivan SD & Castrillon DH 2011 Insights into primary ovarian insufficiency through genetically engineered mouse models. *Semin Reprod Med* **29** 283-298.

Sundin T & Hentosh P 2012 InTERTesting association between telomerase, mTOR and phytochemicals. *Expert Rev Mol Med* **14** e8.

Suter L, Koch E, Bechter R & Bobadilla M 1997 Three-parameter flow cytometric analysis of rat spermatogenesis. *Cytometry* **27** 161-168.

Tarnawa ED, Baker MD, Aloisio GM, Carr BR & Castrillon DH 2013 Gonadal expression of foxo1, but not foxo3, is conserved in diverse Mammalian species. *Biol Reprod* **88** 103.

Tee AR, Blenis J & Proud CG 2005 Analysis of mTOR signaling by the small G-proteins, Rheb and RhebL1. *FEBS Lett* **579** 4763-4768.

Thompson JN, Howell JM & Pitt GA 1964 Vitamin a and Reproduction in Rats. *Proc R Soc Lond B Biol Sci* **159** 510-535.

Tzivion G, Dobson M & Ramakrishnan G 2011 FoxO transcription factors; Regulation by AKT and 14-3-3 proteins. *Biochim Biophys Acta* **1813** 1938-1945.

Vander Haar E, Lee SI, Bandhakavi S, Griffin TJ & Kim DH 2007 Insulin signalling to mTOR mediated by the Akt/PKB substrate PRAS40. *Nat Cell Biol* **9** 316-323.

Wilkins AS & Holliday R 2009 The evolution of meiosis from mitosis. *Genetics* **181** 3-12.

Wolfes H, Kogawa K, Millette CF & Cooper GM 1989 Specific expression of nuclear proto-oncogenes before entry into meiotic prophase of spermatogenesis. *Science* **245** 740-743.

Wolosewick JJ & Bryan JH 1977 Ultrastructural characterization of the manchette microtubules in the seminiferous epithelium of the mouse. *Am J Anat* **150** 301-331.

Wong CH & Cheng CY 2005 The blood-testis barrier: its biology, regulation, and physiological role in spermatogenesis. *Curr Top Dev Biol* **71** 263-296.

Wyrobek AJ & Bruce WR 1975 Chemical induction of sperm abnormalities in mice. *Proc Natl Acad Sci U S A* **72** 4425-4429.

Yaffe MB, Leparc GG, Lai J, Obata T, Volinia S & Cantley LC 2001 A motif-based profile scanning approach for genome-wide prediction of signaling pathways. *Nat Biotechnol* **19** 348-353.

Yan W 2009 Male infertility caused by spermiogenic defects: lessons from gene knockouts. *Mol Cell Endocrinol* **306** 24-32.

Yao HH, Tilmann C, Zhao GQ & Capel B 2002 The battle of the sexes: opposing pathways in sex determination. *Novartis Found Symp* **244** 187-198; discussion 198-206, 253-187.

Yeung CH, Beiglbock-Karau L, Tuttelmann F & Nieschlag E 2007 The presence of germ cells in the semen of azoospermic, cryptozoospermic and severe oligozoospermic patients: stringent flow cytometric analysis and correlations with hormonal status. *Clin Endocrinol (Oxf)* **67** 767-775.

Zhang L, Tang J, Haines CJ, Feng HL, Lai L, Teng X & Han Y 2011 c-kit and its related genes in spermatogonial differentiation. *Spermatogenesis* **1** 186-194.

Zhou C, Gehrig PA, Whang YE & Boggess JF 2003 Rapamycin inhibits telomerase activity by decreasing the hTERT mRNA level in endometrial cancer cells. *Mol Cancer Ther* **2** 789-795.

Zou J, Zhou L, Du XX, Ji Y, Xu J, Tian J, Jiang W, Zou Y, Yu S, Gan L, Luo M, Yang Q, Cui Y, Yang W, Xia X, Chen M, Zhao X, Shen Y, Chen PY, Worley

PF & Xiao B 2011 Rheb1 is required for mTORC1 and myelination in postnatal brain development. *Dev Cell* **20** 97-108.